**Vahab Hassani** et al. "**Fundamentals**"
*Handbook of Heating, Ventilation, and Air Conditioning*
Ed. Jan F. Kreider
Boca Raton, CRC Press LLC. 2001

# 2

# Fundamentals

Vahab Hassani
*National Renewable Energy
Laboratory*

Steve Hauser
*Pacific Northwest
National Laboratory*

T. Agami Reddy
*Drexel University*

## 2.1 Thermodynamics Heat Transfer and Fluid Mechanics Basics

*Vahab Hassani and Steve Hauser*

Design and analysis of energy conversion systems require an in-depth understanding of basic principles of thermodynamics, heat transfer, and fluid mechanics. **Thermodynamics** is that branch of engineering science that describes the relationship and interaction between a system and its surroundings. This interaction usually occurs as a transfer of energy, mass, or momentum between a system and its surroundings. Thermodynamic laws are usually used to predict the changes that occur in a system when moving from one equilibrium state to another. The science of **heat transfer** complements the thermodynamic science by providing additional information about the energy that crosses a system's boundaries. Heat-transfer laws provide information about the mechanism of transfer of energy as heat and provide necessary correlations for calculating the rate of transfer of energy as heat. The science of **fluid mechanics**, one of the most basic engineering sciences, provides governing laws for fluid motion and conditions influencing that motion. The governing laws of fluid mechanics have been developed through a knowledge of fluid properties, thermodynamic laws, basic laws of mechanics, and experimentation.

In this chapter, we will focus on the basic principles of thermodynamics, heat transfer, and fluid mechanics that an engineer needs to know to analyze or design an HVAC system. Because of space limitations, our discussion of important physical concepts will not involve detailed mathematical derivations and proofs of concepts. However, we will provide appropriate references for those readers interested in obtaining more detail about the subjects covered in this chapter. Most of the material presented here is accompanied by examples that we hope will lead to better understanding of the concepts.

### 2.1.1 Thermodynamics

During a typical day, everyone deals with various engineering systems such as automobiles, refrigerators, microwaves, and dishwashers. Each engineering system consists of several components, and a system's optimal performance depends on each individual component's performance and interaction with other components. In most cases, the interaction between various components of a system occurs in the form of energy transfer or mass transfer. Thermodynamics is an engineering science that provides governing

laws that describe energy transfer from one form to another in an engineering system. In this chapter, the basic laws of thermodynamics and their application for energy conversion systems are covered in the following four sections. The efficiency of the thermodynamic cycles and explanations of some advanced thermodynamic systems are presented in the succeeding two sections. Several examples have been presented to illustrate the application of concepts covered here. Because of the importance of moist air HVAC processes, these are treated in Chapter 2.2.

## Energy and the First Law of Thermodynamics

In performing engineering thermodynamic analysis, we must define the *system* under consideration. After properly identifying a thermodynamic system, everything else around the system becomes that system's *environment*. Of interest to engineers and scientists is the *interaction* between the system and its environment.

In thermodynamic analysis, systems can either consist of specified matter (**controlled mass**, CM) or specified space (**control volume**, CV). In a control-mass system, energy—but not mass—can cross the system boundaries while the system is going through a thermodynamic process. Control-mass systems may be called **closed systems** because no mass can cross their boundary. On the other hand, in a control-volume system—also referred to as an **open system**—both energy and matter can cross the system boundaries. The shape and size of CVs need not necessarily be constant and fixed; however, in this chapter, we will assume that the CVs are of fixed shape and size. Another system that should be defined here is an **isolated system**, which is a system where no mass or energy crosses its boundaries.

The energy of a system consists of three components: kinetic energy, potential energy, and internal energy. The **kinetic** and **potential energy** of a system are macroscopically observable. **Internal energy** is associated with random and disorganized aspects of molecules of a system and is not directly observable. In thermodynamic analysis of systems, the energy of the whole system can be obtained by adding the individual energy components.

## Conservation of Energy — The First Law of Thermodynamics

The First Law of Thermodynamics states that energy is conserved: it cannot be created or destroyed, but can change from one form to another. The energy of a closed system can be expressed as

$$E = me + \frac{mu^2}{2g_2} + \frac{mgz}{g_c},$$
(2.1.1)

where $E$ is the total energy of the system, $e$ is its internal energy per unit mass, and the last two terms are the kinetic energy and potential energy of the system, respectively. The proportionality constant $g_c$ is defined in the nomenclature (listed at the end of this chapter) and is discussed in the text following Eq. (2.1.73). When a system undergoes changes, the energy change within the system can be expressed by a general form of the energy-balance equation:

| Energy stored | = | Energy entering | − | Energy leaving | + | Energy generated |
| in the system | | the system | | the system | | in the system |
| | | | | | | (e.g., chemical reactions) |

For example, consider the geothermal-based heat pump shown in Figure 2.1.1. In this heat pump, a working fluid (R-22, a common refrigerant used with geothermal heat pumps, which is gaseous at room temperature and pressure) is sealed in a closed loop and is used as the transport medium for energy. Figure 2.1.2 presents a simple thermodynamic cycle for a heat pump (heating mode) and an associated pressure-enthalpy (p-h) diagram. The saturated vapor and liquid lines are shown in Figure 2.1.2, and the region between these two lines is referred to as the wet region, where vapor and liquid coexist. The relative quantities of liquid and vapor in the mixture, known as the quality of the mixture ($x$), is usually used to denote the state of the mixture. The **quality of a mixture** is defined as the ratio of the mass of vapor to the mass of the mixture. For example, in 1 kg of mixture with quality $x$, there are $x$ kg of vapor
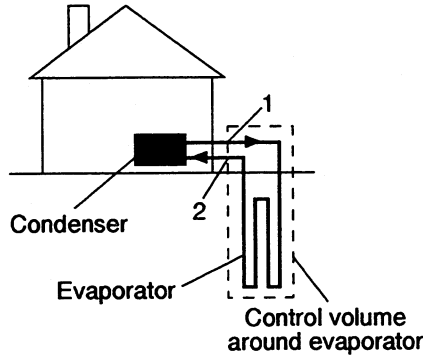
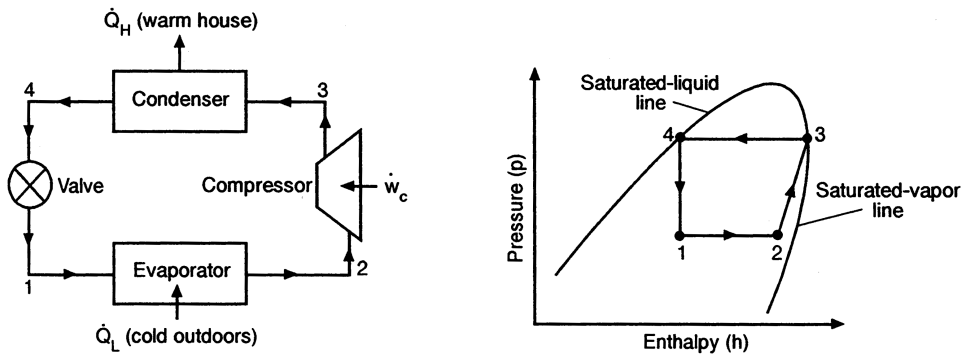**FIGURE 2.1.1** Geothermal-based (ground-source) heat pump.



**FIGURE 2.1.2** Thermodynamic cycle and *p-h* diagram for heat pump (heating mode).

and $(1 - x)$ kg of liquid. Figure 2.1.2 shows that the working fluid leaving the evaporator (point 2) has a higher quality than working fluid entering the evaporator (point 1). The working fluid in Figure 2.1.2 is circulated through the closed loop and undergoes several phase changes. Within the evaporator, the working fluid absorbs heat from the surroundings (geothermal resource) and is vaporized. The low-pressure gas (point 2) is then directed into the compressor, where its pressure and temperature are increased by compression. The hot compressed gas (point 3) is then passed through the condenser, where it loses heat to the surroundings (heating up the house). The cool working fluid exiting the condenser is a high-pressure liquid (point 4), which then passes through an expansion device or valve to reduce its pressure to that of the evaporator (underground loop).

Specifically, consider the flow of the working fluid in Figure 2.1.1 from point 1 to point 2 through the system shown within the dashed rectangle. Mass can enter and exit this control-volume system. In flowing from point 1 to 2, the working fluid goes through the evaporator (see Figure 2.1.2). Assuming no accumulation of mass or energy, the First Law of Thermodynamics can be written as

$$e_2 + \frac{u_2^2}{2g_c} + \frac{gz_2}{g_c} + p_2v_2 = e_1 + \frac{u_1^2}{2g_c} + \frac{gz_1}{g_c} + p_1v_1 + \frac{\dot{Q} - \dot{w}}{\dot{m}}, \qquad (2.1.2)$$

where $\dot{m}$ is the mass-flow rate of the working fluid, $\dot{Q}$ is the rate of heat absorbed by the working fluid, $\dot{w}$ is the rate of work done on the surroundings, $v$ is the specific volume of the fluid, $p$ is the pressure, and the subscripts 1 and 2 refer to points 1 and 2. A mass-flow energy-transport term, $pv$, appears in Eq. (2.1.2) as a result of our choice of control-volume system. The terms $e$ and $pv$ can be combined into a single term called **specific enthalpy**, $h = e + pv$, and Eq. (2.1.2) then reduces to

$$\frac{1}{2g_c}\left(u_2^2 - u_1^2\right) + \frac{g}{g_c}\Delta z_{2-1} + \Delta h_{2-1} = \frac{\dot{Q} - \dot{w}}{\dot{m}}. \tag{2.1.3}$$

For a constant-pressure process, the enthalpy change from temperature, $T_1$ to temperature $T_2$ can be expressed as

$$\Delta h_{2-1} = \int_{T_1}^{T_2} c_p \ dT = \bar{c}_p\left(T_2 - T_1\right), \tag{2.1.4}$$

where $\bar{c}_p$ is the mean specific heat at constant pressure.

### Entropy and the Second Law of Thermodynamics

In many events, the state of an isolated system can change in a given direction, whereas the reverse process is impossible. For example, the reaction of oxygen and hydrogen will readily produce water, whereas the reverse reaction (electrolysis) cannot occur without some external help. Another example is that of adding milk to hot coffee. As soon as the milk is added to the coffee, the reverse action is impossible to achieve. These events are explained by the Second Law of Thermodynamics, which provides the necessary tools to rule out impossible processes by analyzing the events occurring around us with respect to time. Contrary to the First Law of Thermodynamics, the Second Law is sensitive to the *direction* of the process.

To better understand the second law of thermodynamics, we must introduce a thermodynamic property called **entropy** (symbolized by $S$, representing total entropy, and $s$, representing entropy per unit mass). The entropy of a system is simply a measure of the degree of molecular chaos or disorder at the microscopic level within a system.

The more disorganized a system is, the less energy is available to do useful work; in other words, energy is required to create order in a system. When a system goes through a thermodynamic process, the natural state of affairs dictates that entropy be produced by that process. In essence, the Second Law of Thermodynamics states that, in an isolated system, entropy can be produced, but it can never be destroyed.

$$\Delta S = S_{\text{final}} - S_{\text{initial}} \geq 0 \quad \text{for isolated system.} \tag{2.1.5}$$

Thermodynamic processes can be classified as reversible and irreversible processes. A **reversible process** is a process during which the net entropy of the system remains unchanged. A reversible process has equal chances of occurring in either a forward or backward direction because the net entropy remains unchanged. The absolute incremental entropy change for a closed system of fixed mass in a reversible process can be calculated from

$$dS = \frac{dQ}{T}, \tag{2.1.6}$$

where $dS$ is the increase in entropy, $dQ$ is the heat absorbed, and $T$ is the absolute temperature. However, the net change in entropy for all the participating systems in the reversible process must equal zero; thus,

$$\Delta S = \sum_{\text{all systems}} dS = \sum_{\text{all systems}} \frac{dQ}{T} = 0. \tag{2.1.7}$$

We emphasize that most real processes are not reversible and the entropy of a real process is not usually conserved. Therefore, Eq. (2.1.6) can be written in a general form as
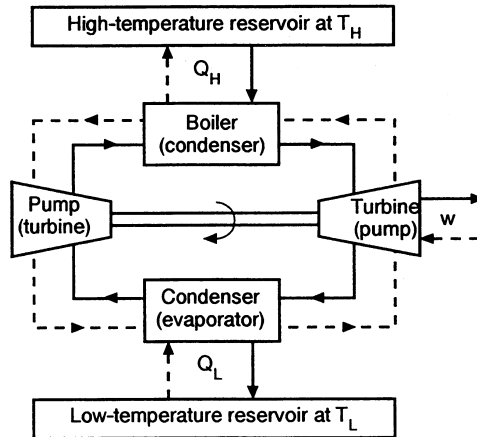
**FIGURE 2.1.3**   Principle of operation of a heat engine (solid lines and upper terms) and heat pump (dashed lines and lower terms in parentheses).

$$dS \geq \frac{dQ}{T}, \tag{2.1.8}$$

where the equality represents the reversible process. A reversible process in which $dQ = 0$ is called an **isentropic process**. It is obvious from Eq. (2.1.6) that for such processes, $dS = 0$, which means that no net change occurs in the entropy of the system or its surroundings.

### Application of the Thermodynamic Laws to HVAC and Other Energy Conversion Systems

We can now employ these thermodynamic laws to analyze thermodynamic processes that occur in energy conversion systems. Among the most common energy conversion systems are heat engines and heat pumps. In Figure 2.1.3, the *solid* lines indicate the operating principle of a **heat engine**, where energy $Q_H$, is absorbed from a high-temperature thermal reservoir and is converted to work $w$ by using a turbine, and the remainder, $Q_L$, is rejected to a low-temperature thermal reservoir. The **energy-conversion efficiency** of a heat engine is defined as

$$\eta_{\text{heat engine}} = \frac{\text{desired output energy}}{\text{required input energy}} = \frac{w}{Q_H}. \tag{2.1.9}$$

In the early 1800s, Nicholas Carnot showed that to achieve the maximum possible efficiency, the heat engine must be completely reversible (i.e., no entropy production, no thermal losses due to friction). Using Eq. (2.1.7), Carnot's heat engine should give

$$\Delta S = \frac{Q_H}{T_H} - \frac{Q_L}{T_L} = 0 \tag{2.1.10}$$

or

$$\frac{Q_H}{Q_L} = \frac{T_H}{T_L}. \tag{2.1.11}$$

An energy balance gives

$$w = Q_H - Q_L. \tag{2.1.12}$$

Therefore, the maximum possible efficiency is

$$\eta_{rev} = \frac{Q_H - Q_L}{Q_H} = 1 - \frac{Q_L}{Q_H} = 1 - \frac{T_L}{T_H}. \qquad (2.1.13)$$

In real processes, however, due to entropy production, the efficiency is

$$\eta \leq 1 - \frac{T_L}{T_H}. \qquad (2.1.14)$$

A **heat pump** is basically a heat engine with the reverse thermodynamic process. In heat pumps, work input allows for thermal energy transfer from a low-temperature reservoir to a high-temperature reservoir as shown in Figure 2.1.3 by *dashed* lines. Energy (heat), $Q_L$, is absorbed by a working fluid from a low-temperature reservoir (geothermal resource or solar collectors), then the energy content (temperature and pressure) of the working fluid is increased as a result of input work, $w$. The energy, $Q_H$, of the working fluid is then released to a high-temperature reservoir (e.g., a warm house). The efficiency of a heat pump is defined as

$$\eta_{heat\ pump} = \frac{\text{desired output energy}}{\text{required input energy}} = \frac{Q_H}{w} = \frac{Q_H}{Q_H - Q_L}. \qquad (2.1.15)$$

The efficiency of a heat pump is often expressed as **coefficient of performance** (COP). The COP of a Carnot (or reversible) heat pump can be expressed as

$$COP = \frac{T_H}{T_H - T_L}. \qquad (2.1.16)$$

Heat pumps are often used in HVAC systems to heat or cool buildings. Heat engines and heat pumps are broadly discussed by Sandord [1962], Reynolds and Perkins [1977], Wood [1982], Karlekar [1983], and Van Wylen and Sonntag [1986].

### Efficiencies of Thermodynamic Cycles

To evaluate and compare various thermodynamic cycles (or systems), we further define and employ the term *efficiency*. The operating efficiency of a system reflects irreversibilities that exist in the system. To portray various deficiencies or irreversibilities of existing thermodynamic cycles, the following thermodynamic efficiency terms are most commonly considered.

$$\text{Mechanical efficiency} \quad \eta_m = \frac{w_{act}}{w_{rev}}, \qquad (2.1.17)$$

which is the ratio of the actual work produced by a system to that of the same system under reversible process. Note that the reversible process is not necessarily an adiabatic process (which would involve heat transfer across the boundaries of the system).

$$\text{Isentropic Efficiency} \quad \eta_s = \frac{w_{act}}{w_{isent}}, \qquad (2.1.18)$$

which is the ratio of actual work to the work done under an isentropic process.

$$\text{Relative efficiency} \quad \eta_r = \frac{w_{rev}}{w_{isent}}, \qquad (2.1.19)$$

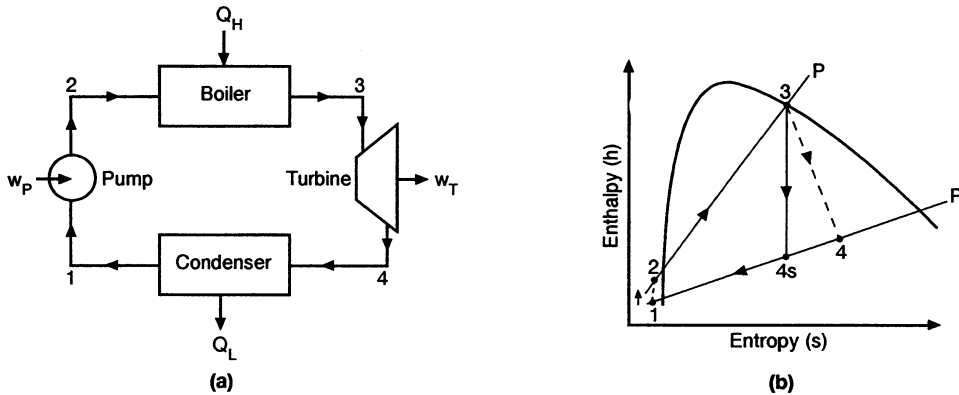**FIGURE 2.1.4**    Typical Rankine cycle and its *h-s* diagram.

which is the ratio of reversible work to isentropic work.

$$\text{Thermal efficiency} \quad \eta_T = \frac{\dot{w}_{\text{out}}}{\dot{Q}_{\text{in}}}, \qquad (2.1.20)$$

which is the ratio of the net power output to the input heat rate. Balmer [1990] gives a comprehensive discussion on the efficiency of thermodynamic cycles.

### Some Thermodynamic Systems

The most common thermodynamic systems are those used by engineers in generating electricity for utilities and for heating or refrigeration/cooling purposes.

Modern power systems employ after Rankine cycles, and a typical **Rankine cycle** is shown in Figure 2.1.4(a). In this cycle, the working fluid is compressed by the pump and is sent to the boiler where heat $Q_H$ is added to the working fluid, bringing it to a saturated (or superheated) vapor state. The vapor is then expanded through the turbine, generating shaft work. The mixture of vapor and liquid exiting the turbine is condensed by passing through the condenser. The fluid coming out of the condenser is then pumped to the boiler, closing the cycle. The enthalpy-entropy (h-s) diagram for the Rankine cycle is shown in Figure 2.1.4(b). The dashed line 3→4 in Figure 2.1.4(b) represents actual expansion of the steam through the turbine, whereas the solid line 3→4*s* represents an isentropic expansion through the turbine.

In utility power plants, the heat source for the boiler can vary depending on the type of generating plant. In geothermal power plants, for example, water at temperatures as high as 380°C is pumped from geothermal resources located several hundred meters below the earth's surface, and the water's energy is transferred to the working fluid in a boiler.

The other commonly used thermodynamic cycle is the **refrigeration cycle** (heat-pump cycle). As stated earlier, a heat engine and a heat pump both operate under the same principles except that their thermodynamic processes are reversed. Figures 2.1.2 and 2.1.3 provide detailed information about the heat-pump cycle. This cycle is sometimes called the reversed Rankine cycle.

### *Modified Rankine Cycles*

Modifying the Rankine cycle can improve the output work considerably. One modification usually employed in large central power stations is introducing a **reheat process** into the Rankine cycle. In this modified Rankine cycle, as shown in Figure 2.1.5(a), steam is first expanded through the first stage of the turbine. The steam discharging from the first stage of the turbine is then reheated before entering the second stage of the turbine. The reheat process allows the second stage of the turbine to have a greater enthalpy change. The enthalpy-versus-entropy plot for this cycle is shown in Figure 2.1.5(b), and this figure should be compared to Figure 2.1.4(b) to further appreciate the effect of the reheat process. Note
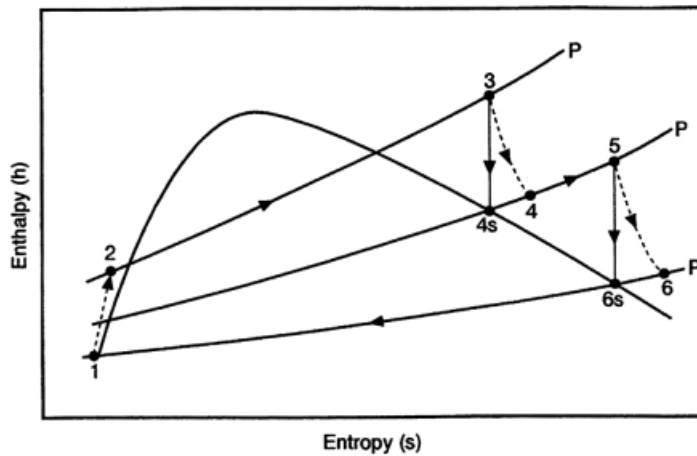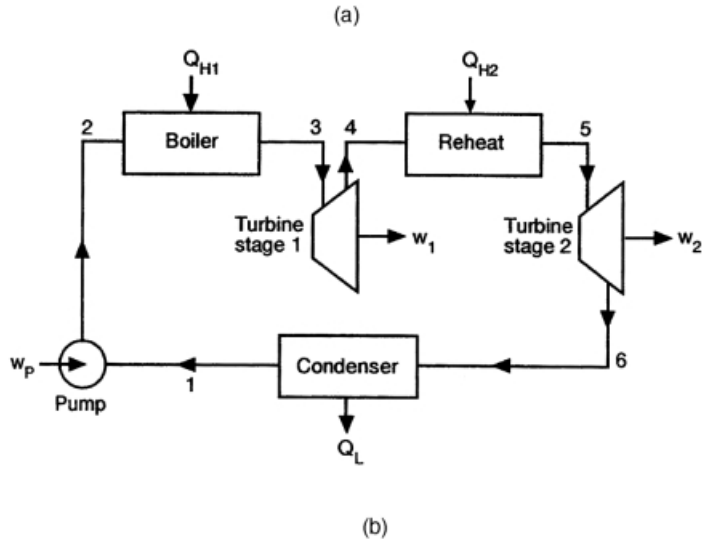
FIGURE 2.1.5 (a) Rankine cycle with a reheat process. (b) The *h-s* plot for the modified Rankine cycle of Figure 2.1.5(a).

that in the reheat process, the work output per pound of steam increases; however, the efficiency of the system may be increased or reduced depending on the reheat temperature range.

Another modification also employed at large power stations is called a **regeneration process**. The schematic representation of a Rankine cycle with a regeneration process is shown in Figure 2.1.6(a), and the enthalpy-versus-entropy plot is shown in Figure 2.1.6(b). In this process, a portion of the steam (at point 6) that has already expanded through the first stage of the turbine is extracted and is mixed in an open regenerator with the low-temperature liquid (from point 2) that is pumped from the condenser back to the boiler. The liquid coming out of the regenerator at point 3 is saturated liquid that is then pumped to the boiler.

### Example 2.1.1

A geothermal heat pump, shown in Figure 2.1.7, keeps a house at 24°C during the winter. The geothermal resource temperature is –5°C. The amount of work required to operate the heat pump for a particular month is $10^6$ kilojoules (kJ). What is the maximum heat input to the house during that 1-month period?
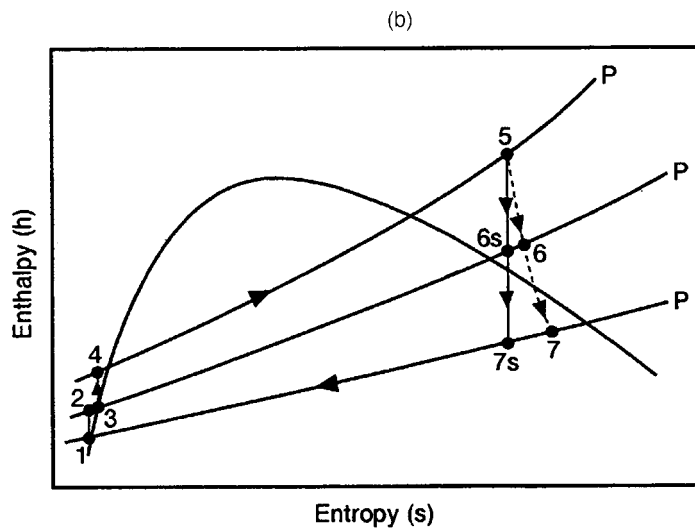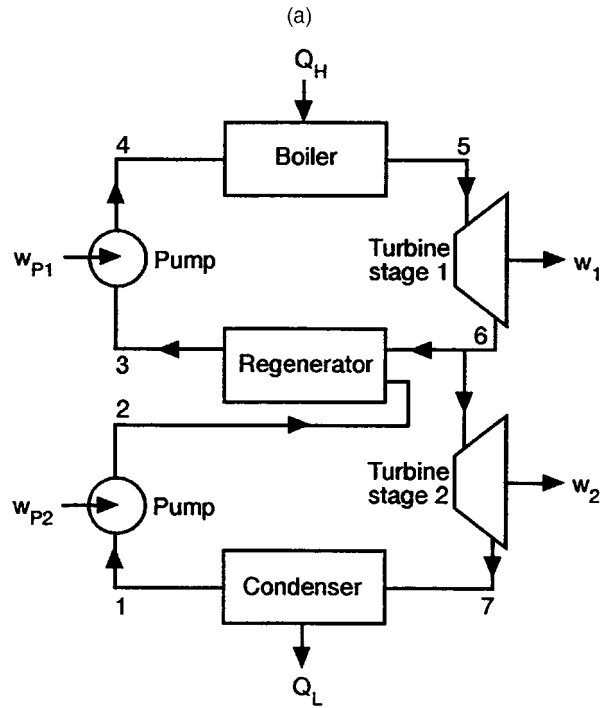
FIGURE 2.1.6   (a) Rankine cycle with regeneration process, and (b) its *h-s* diagram.

*Solution:*

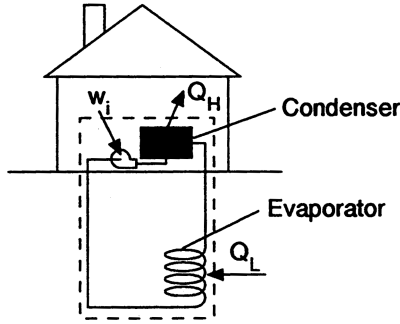The energy balance for the system gives

$$w_i + Q_L = Q_H. \tag{2.1.21}$$

**FIGURE 2.1.7**   Ground-source heat pump.

Equation (2.1.7) gives the entropy change for the system:

$$\Delta S = \frac{Q_H}{T_H} - \frac{Q_L}{T_L},$$

(2.1.22)

where, from Eq. (2.1.22), we can get an expression for $Q_L$:

$$Q_L = \frac{Q_H T_L}{T_H} - T_L \Delta S.$$

(2.1.23)

Substituting for $Q_L$ from Eq. (2.1.21), we get an expression for $Q_H$:

$$Q_H = \frac{1}{1 - \dfrac{T_L}{T_H}} \left( w_i - T_L \Delta S \right).$$

The maximum $Q_H$ is obtained when $\Delta S = 0$; therefore,

$$Q_H \leq \frac{1}{1 - \dfrac{T_L}{T_H}}\; w_i,$$

(2.1.24)

and substituting the actual values yields

$$Q_H \leq \frac{1}{1 - \dfrac{268.15\ \text{K}}{297.15\ \text{K}}} \times 10^6\ kJ,\ or\ Q_H \leq 10^7\ kJ.$$

*Example 2.1.2*

Calculate the maximum COP for the heat pump of Example 2.1.1.

Solution

$$COP_{\text{heat pump}} = \frac{Q_H}{Q_H - Q_L} = \frac{10^7\ kJ}{10^6\ kJ} = 10.$$

*Example 2.1.3*

A simple heat-pump system is shown in Figure 2.1.2. The working fluid in the closed loop is R-22. The p-h diagram of Figure 2.1.2 shows the thermodynamic process for the working fluid. The following data represent a typical operating case.

$$T_1 = T_2 = -5°C \ (23°F)$$

$$T_3 = T_4 = 24°C \ (75°F)$$

$$x_1 = 0.17$$

(a) Determine the COP for this heat pump assuming isentropic compression, $s_2 = s_3$.

(b) Determine the COP by assuming a compressor isentropic efficiency of 70%.

*Solution:*

First, the thermodynamic properties at each station can be found using the *CRC Mechanical Engineer's Handbook*.

*State Point #1:*

The evaporation of working fluid R-22 occurs at a constant pressure (between points 1 and 2). This pressure can be obtained from the saturated liquid/vapor table of properties for R-22 at $T_1 = -5°C$ (23°F), which is $p_1 = 422$ kPa (61.2 psia). At point 1, the quality is $x_1 = 0.17$. Therefore, the enthalpy and entropy at this point can be obtained from:

$$h_1 = h_{f_1} + x_1 \ h_{fg_1} \quad \text{and} \quad s_1 = s_{f_1} + x \ s_{fg_1},$$

where $h_{f_1} = 39.36$ kJ/kg, $h_{fg_1} - h_{f_1} = h_{g_1} = 208.85$ kJ/kg, $s_{f_1} = 0.1563$ kJ/kg K, and $s_{fg_1} = s_{g_1} - s_{f_1} = 0.7791$ kJ/kg K.

The quantities listed are read from the table of properties for R-22. Using these properties, we obtain:

$$h_1 = 39.36 \text{ kJ/kg} + 0.17 \ (208.85 \text{ kJ/kg}) = 74.86 \text{ kJ/kg},$$

$$s_1 = 0.1563 \text{ kJ/kg K} + 0.17 \ (0.7791 \text{ kJ/kg K}) = 0.2887 \text{ kJ/kg K}$$

We then find the state properties at point 3, because they will be used to find the quality of the mixture at point 2.

*State Point #3:*

At point 3, the working fluid is saturated vapor at $T_3 = 24°C$ (75°F). From the table of properties, the pressure, enthalpy, and entropy at this point are $p_3 = 1{,}014$ kPa (147 psia), $h_3 = 257.73$ kJ/kg, and $s_3 = 0.8957$ kJ/kg K.

*State Point #2:*

The temperature at this point is $T_2 = -5°C$ (23°F), and because we are assuming an isentropic compression, the entropy is $s_2 = s_3 = 0.8957$ kJ/kg K. The quality of the mixture at point 2 can be calculated from

$$x_2 = \frac{s_2 - s_{f_2}}{s_{fg_2}},$$

where $s_{fg_2} = s_{g_2} - s_{f_2}$, and the quantities $s_{g_2}$ and $s_{f_2}$ can be obtained from the table of properties at $T_2 = -5°C$ (23°F).

Note that the saturation properties for points 1 and 2 are the same because both points have the same pressure and temperature. Therefore,

$$s_{f_2} = s_{f_1} = 0.1563 \text{ kJ/kg K},$$

$$h_{f_2} = h_{f_1} = 39.36 \text{ kJ/kg},$$

$$s_{fg_2} = s_{fg_1} = 0.7791 \text{ kJ/kg K},$$

$$h_{fg_2} = h_{fg_1} = 208.85 \text{ kJ/kg},$$

$$s_2 = \frac{s_2 - s_{f_2}}{s_{fg_2}} = \frac{0.8957 \text{ kJ/kg K} - 0.1563 \text{ kJ/kg K}}{0.7791 \text{ kJ/kg K}} = 0.95.$$

Knowing the quality at point 2, the enthalpy at point 2 can be calculated:

$$h_2 = h_{f_2} + x_2 \; h_{fg_2} = 39.36 \text{ kJ/kg} + 0.95 \left(208.85 \text{ kJ/kg}\right) = 237.77 \text{ kJ/kg}.$$

### State Point #4

At point 4, we have saturated liquid at $T_4 = 24°C$ (75°F). Therefore, from the table of properties, $s_4 = 0.2778$ kJ/kg K and $h_4 = 74.16$ kJ/kg.

(a) The coefficient of performance for a heat pump is

$$\text{COP} = \frac{\text{rate of energy transfer to house}}{\text{compressor shaft power}}$$

$$= \frac{h_3 - h_4}{h_3 - h_2} = \frac{183.57 \text{ kJ/kg}}{19.96 \text{ kJ/kg}} = 9.2.$$

(b) If the isentropic efficiency is 70%, the *p-h* diagram is as shown in Figure 2.1.8. The isentropic efficiency for the compressor is defined as

$$h_s = \frac{h_{3s} - h_2}{h_3 - h_2}.$$
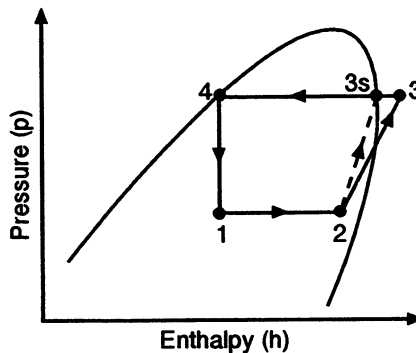


**FIGURE 2.1.8**    The *p-h* diagram for a heat-pump cycle with a 70% isentropic efficiency for the compressor.
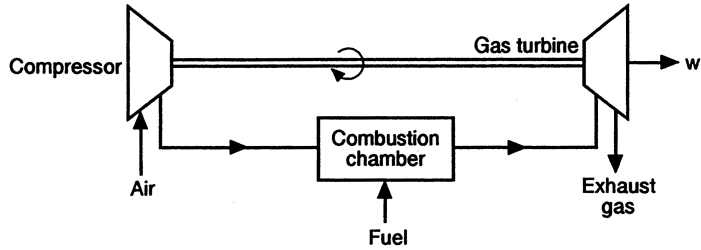
**FIGURE 2.1.9**  A basic gas-turbine or Brayton-cycle representation.

Using this relationship, $h_3$ can be calculated as follows:

$$h_3 = \frac{h_{3s} - h_2}{\eta_s} + h_2 = \frac{257.73 \text{ kJ/kg} - 237.77 \text{ kJ/kg}}{0.70} + 237.77 \text{ kJ/kg} = 266.28 \text{ kJ/kg}.$$

Therefore, the COP is

$$COP = \frac{h_3 - h_4}{h_3 - h_2} = \frac{266.28 \text{ kJ/kg} - 74.16 \text{ kJ/kg}}{266.28 \text{ kJ/kg} - 237.77 \text{ kJ/kg}} = 6.7.$$

*Advanced Thermodynamic Power Cycles*

Over the past 50 years, many technological advances have improved the performance of power plant components. Recent developments in exotic materials have allowed the design of turbines that can operate more efficiently at higher inlet temperatures and pressures. Simultaneously, innovative thermodynamic technologies (processes) have been proposed and implemented that take advantage of improved turbine isentropic and mechanical efficiencies and allow actual operating thermal efficiencies of a power station to approach 50%. These improved technologies include (1) modification of existing cycles (reheat and regeneration) and (2) use of combined cycles. In the previous section, we discussed reheat and regeneration techniques. In the following paragraphs, we give a short overview of the combined-cycle technologies and discuss their operation.

The basic gas-turbine or **Brayton cycle** is shown in Figure 2.1.9. In this cycle, ambient air is pressurized in a compressor and the compressed air is then forwarded to a combustion chamber, where fuel is continuously supplied and burned to heat the air. The combustion gases are then expanded through a turbine to generate mechanical work. The turbine output runs the air compressor and a generator that produces electricity.

The exhaust gas from such a turbine is very hot and can be used in a bottoming cycle added to the basic gas-turbine cycle to form a **combined cycle**. Figure 2.1.10 depicts such a combined cycle where a **heat-recovery steam generator** (HRSG) is used to generate steam required for the bottoming (Rankine)
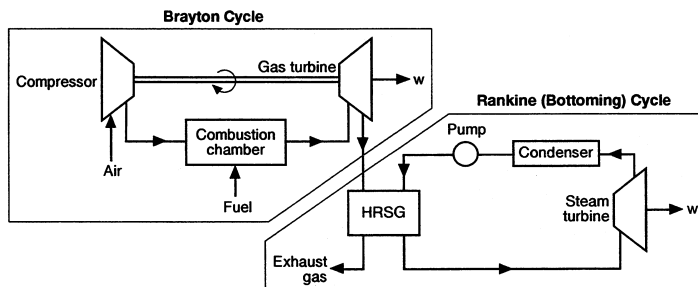


**FIGURE 2.1.10**  A combined cycle known as the steam-and-gas-turbine cycle.

cycle. The high-temperature exhaust gases from the gas-turbine (Brayton) cycle generate steam in the HRSG. The steam is then expanded through the steam turbine and condensed in the condenser. Finally, the condensed liquid is pumped to the HRSG for heating. This combined cycle is referred to as a **steam and gas turbine cycle**.

Another type of bottoming cycle proposed by Kalina [1984] uses a mixture of ammonia and water as a working fluid. The multicomponent mixture provides a boiling process that does not occur at a constant temperature; as a result, the available heat is used more efficiently. In addition, Kalina employs a distillation process or working-fluid preparation subsystem that uses the low-temperature heat available from the mixed-fluid turbine outlet. The working-fluid mixture is enriched by the high-boiling-point component; consequently, condensation occurs at a relatively constant temperature and provides a greater pressure drop across the turbine. The use of multicomponent working fluids in Rankine cycles provides variable-temperature boiling; however, the condensation process will have a variable temperature as well, resulting in system inefficiencies. According to Kalina, this type of bottoming cycle increases the overall system efficiency by up to 20% above the efficiency of the combined-cycle system using a Rankine bottoming cycle. The combination of the cycle proposed by Kalina and a conventional gas turbine is estimated to yield thermal efficiencies in the 50 to 52% range.

## 2.1.2   Fundamentals of Heat Transfer

In Section 2.1, we discussed thermodynamic laws and through some examples we showed that these laws are concerned with interaction between a system and its environment. Thermodynamic laws are always concerned with the **equilibrium** state of a system and are used to determine the amount of energy required for a system to change from one equilibrium state to another. These laws do not quantify the mode of the energy transfer or its rate. Heat transfer relations, however, complement thermodynamic laws by providing **rate equations** that relate the heat transfer rate between a system and its environment.

Heat transfer is an important process that is an integral part of our environment and daily life. The heat-transfer or heat-exchange process between two media occurs as a result of a temperature difference between them. Heat can be transferred by three distinct modes: conduction, convection, and radiation. Each one of these heat transfer modes can be defined by an appropriate rate equation presented below:

**Fourier's Law of Heat Conduction**—represented here by Eq. (2.1.25) for the one-dimensional steady-state case:

$$\dot{Q}_{\text{cond}} = -kA\frac{dT}{dx}.$$

(2.1.25)

**Newton's Law of Cooling**—which gives the rate of heat transfer between a surface and a fluid:

$$\dot{Q}_{\text{conv}} = hA\,\Delta T,$$

(2.1.26)

where h is the average heat-transfer coefficient over the surface with area $A$.

**Stefan–Boltzmann's Law of Radiation**—which is expressed by the equation:

$$\dot{Q}_r = A_1 F_{1-2}\,\sigma\left(T_1^4 - T_2^4\right).$$

(2.1.27)

## Conduction Heat Transfer

Conduction is the heat-transfer process that occurs in solids, liquids, and gases through molecular interaction as a result of a temperature gradient. The energy transfer between adjacent molecules occurs without significant physical displacement of the molecules. The rate of heat transfer by conduction can be predicted by using Fourier's law, where the effect of molecular interaction in the heat-transfer medium
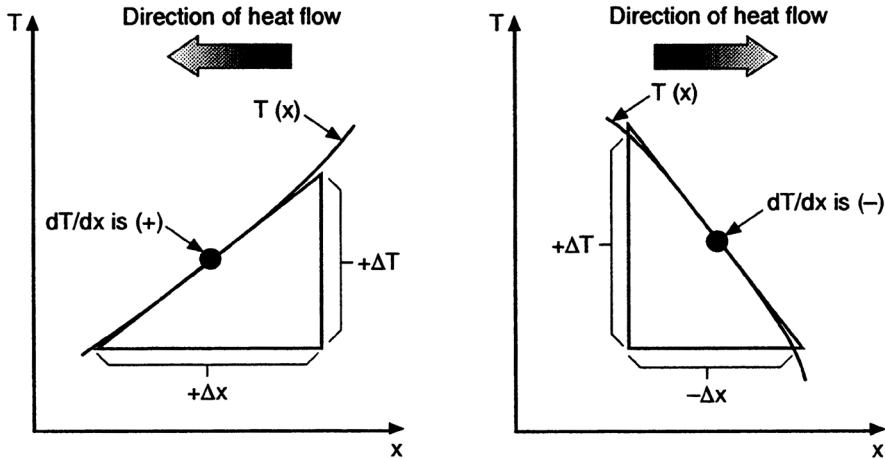
**FIGURE 2.1.11**    The sign convention for conduction heat flow.

is expressed as a property of that medium and is called the **thermal conductivity**. The study of conduction heat transfer is a well-developed field where sophisticated analytical and numerical techniques are used to solve many problems in buildings including heating and cooling load calculation.

In this section, we discuss basics of steady-state one-dimensional conduction heat transfer through homogeneous media in cartesian and cylindrical coordinates. Some examples are provided to show the application of the fundamentals presented, and we also discuss fins or extended surfaces.

### *One-Dimensional Steady-State Heat Conduction*

Fourier's law, as represented by Eq. (2.1.25), states that the rate of heat transferred by conduction is directly proportional to the temperature gradient and the surface area through which the heat is flowing.

The proportionality constant $k$ is the thermal conductivity of the heat-transfer medium. Thermal conductivity is a thermophysical property and has units of W/m K in the SI system, or Btu/h ft °F in the English system of units. Thermal conductivity can vary with temperature, but for most materials it can be approximated as a constant over a limited temperature range. A graphical representation of Fourier's law is shown in Figure 2.1.11.

Equation (2.1.25) is only used to calculate the rate of heat conduction through a one-dimensional homogenous medium (uniform $k$ throughout the medium). Figure 2.1.12 shows a section of a plane wall with thickness $L$, where we assume the other two dimensions of the wall are very large compared to $L$. One side of the wall is at temperature $T_1$, and the other side is kept at temperature $T_2$, where $T_1 > T_2$. Integrating Fourier's law with constant $k$ and $A$, the rate of heat transfer through this wall is

$$\dot{Q} = kA \frac{T_1 - T_2}{L}, \qquad (2.1.28)$$

where $k$ is the thermal conductivity of the wall.

### *The Concept of Thermal Resistance*

Figure 2.1.12 also shows the analogy between electrical and thermal circuits. Consider an electric current $I$ flowing through a resistance $R_e$, as shown in Figure 2.1.12. The voltage difference $\Delta V = V_1 - V_2$ is the driving force for the flow of electricity. The electric current can then be calculated from

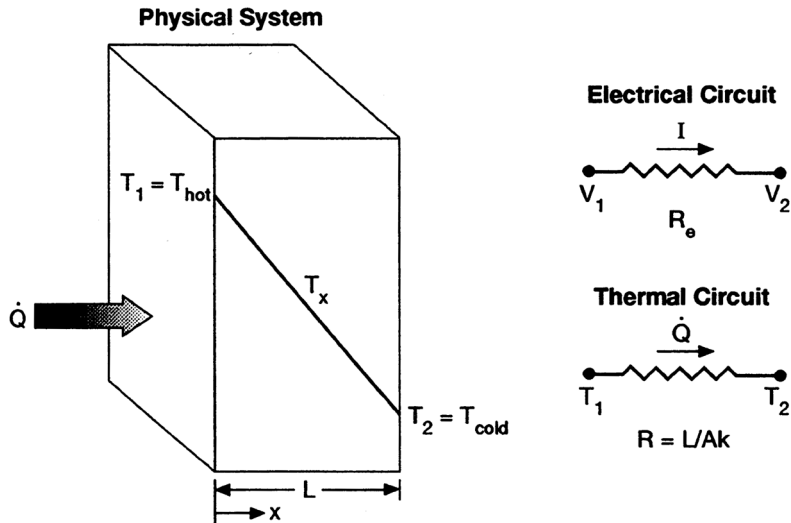$$I = \frac{\Delta V}{R_e}. \qquad (2.1.29)$$

**FIGURE 2.1.12** Analogy between thermal and electrical circuits for steady-state conduction through a plane wall.

Like electric current flow, heat flow is governed by the temperature difference, and it can be calculated from

$$\dot{Q} = \frac{\Delta T}{R},\tag{2.1.30}$$

where, from Eq. (2.1.28), $R = L/Ak$ and is called **thermal resistance**. Following this definition, the thermal resistance for convection heat transfer given by Newton's Law of Cooling becomes $R = 1/(hA)$. Thermal resistance of composite walls (plane and cylindrical) has been discussed by Kakac and Yener [1988], Kreith and Bohn [1993], and Bejan [1993]. The following example shows how we can use the concept of thermal resistance in solving heat-transfer problems in buildings.

*Example 2.1.4*

One wall of an uninsulated house, shown in Figure 2.1.13, has a thickness of 0.30 m and a surface area of 11 m$^2$. The wall is constructed from a material (brick) that has a thermal conductivity of 0.55 W/m K. The outside temperature is –10°C, while the house temperature is kept at 22°C. The convection heat-transfer coefficient is estimated to be $h_o = 21$ W/m$^2$ K in the outside and $h_i = 7$ W/m$^2$ K in the inside. Calculate the rate of heat transfer through the wall, as well as the surface temperature at either side of the wall.

*Solution:*

The conduction thermal resistance is

$$R_{t,\text{cond}} = \frac{L}{Ak} = \frac{0.3 \ \text{m}}{11 \ \text{m}^2 \times 0.55 \ \text{W/m K}} = 0.0496 \frac{\text{K}}{\text{W}}.$$

Note that the heat-transfer rate per unit area is called **heat flux** and is given by

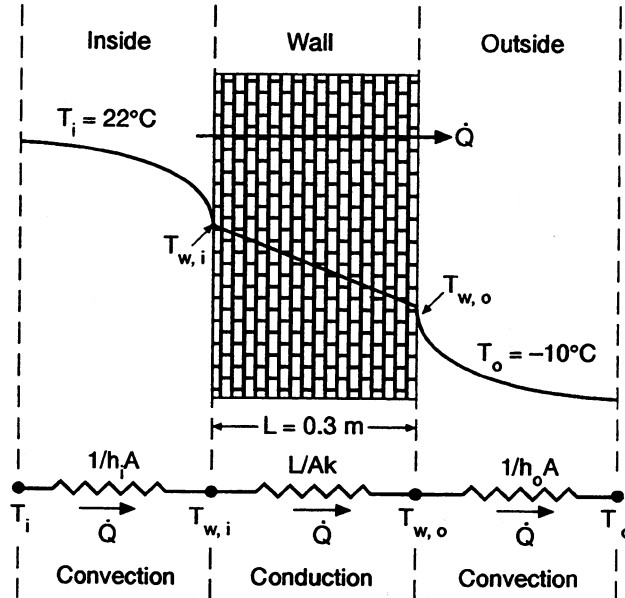$$q'' = \frac{\dot{Q}}{A} = \frac{T_1 - T_2}{L/k}.$$

**FIGURE 2.1.13**    Heat loss through a plane wall.

In this case, the resistance to heat transfer over a 1–m by 1–m area of the wall is

$$R_{t,\text{cond}} = L/k = \frac{0.3 \text{ m}}{0.55 \text{ W/m K}} = 0.5455 \frac{\text{m}^2 \text{ K}}{\text{W}}.$$

The convection resistances for inside and outside, shown in Figure 2.1.13, are

$$R_{i,\text{conv}} = \frac{1}{h_i A} = \frac{1}{7 \text{ W/m}^2 \text{ K} \times 11 \text{ m}^2} = 0.0130 \frac{\text{K}}{\text{W}}$$

$$R_{o,\text{conv}} = \frac{1}{h_o A} = \frac{1}{21 \text{ W/m}^2 \text{ K} \times 11 \text{ m}^2} = 0.0043 \frac{\text{K}}{\text{W}}.$$

Note that the highest resistance is provided by conduction through the wall. The total heat flow can be calculated from

$$\dot{Q} = \frac{\Delta T}{\Sigma R} = \frac{T_i - T_o}{\dfrac{1}{h_i A} + \dfrac{L}{kA} + \dfrac{1}{h_o A}} = \frac{295.15 \text{ K} - 263.15 \text{ K}}{0.013 \dfrac{\text{K}}{\text{W}} + 0.0496 \dfrac{\text{K}}{\text{W}} + 0.0043 \dfrac{\text{K}}{\text{W}}} = 478.3 \text{ W}.$$

The surface temperatures can then be calculated by using the electric analogy depicted in Figure 2.1.13. For the inside surface temperature,

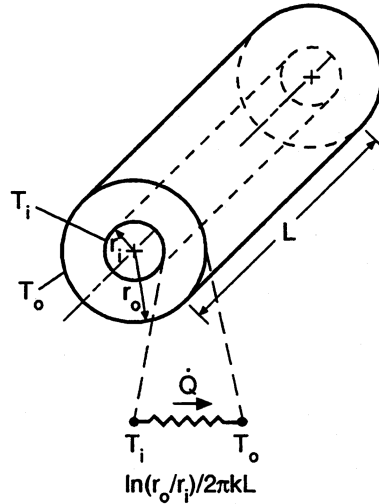$$\dot{Q} = \frac{T_i - T_{w,i}}{\dfrac{1}{h_i A}},$$

**FIGURE 2.1.14**   Conduction through hollow cylinders.

or

$$T_{w,i} = T_i - \frac{\dot{Q}}{h_i A} = 295.15 \text{ K} - \frac{478.3 \text{ W}}{77 \text{ W/K}} = 288.94 \text{ K} = 15.79°C.$$

Similarly, for the outside surface temperature:

$$T_{w,o} = \frac{\dot{Q}}{h_o A} + T_o = \frac{478.3 \text{ W}}{231 \text{ W/K}} + 263.15 \text{ K} = 265.22 \text{ K} = -7.93°C.$$

### Conduction Through Hollow Cylinders

A cross section of a long hollow cylinder such as pipe insulation with internal radius $r_i$ and external radius $r_o$ is shown in Figure 2.1.14. The internal surface of the cylinder is at temperature $T_i$ and the external surface is at $T_o$, where $T_i > T_o$. The rate of heat conduction in a radial direction is calculated by

$$\dot{Q} = \frac{2\pi L k (T_i - T_o)}{\ln(r_o/r_i)},$$

(2.1.31)

where L is the length of the cylinder that is assumed to be long enough so that the end effects may be ignored. From Eq. (2.1.31) the resistance to heat flow in this case is

$$R = \frac{\ln(r_o/r_i)}{2\pi k L}.$$

(2.1.32)

Equation (2.1.31) can be used to calculate the heat loss through insulated pipes, as presented in the following example.

### Example 2.1.5

The refrigerant of the heat pump discussed in Example 2.1.3 is circulating through a thin-walled copper tube of radius $r_i = 6$ mm, as shown in Figure 2.1.15. The refrigerant temperature is $T_i$, ambient temperature is $T_\infty$, and $T_i < T_\infty$. The outside convection heat-transfer coefficient is $h_o = 7$ W/m² K.
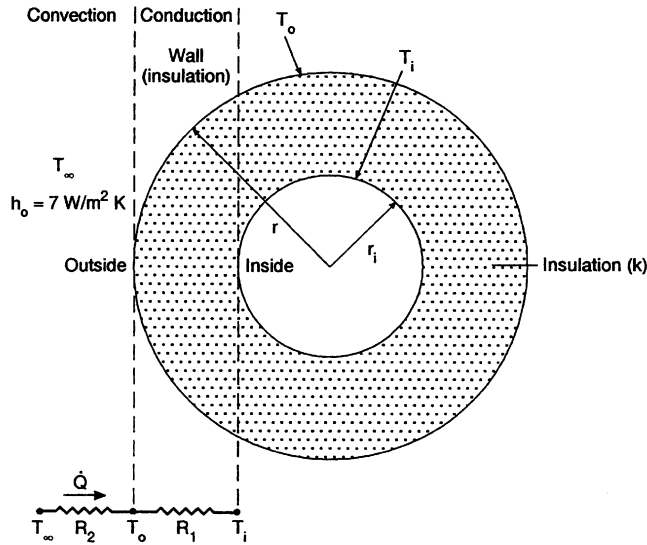
**FIGURE 2.1.15** Heat loss through a pipe with insulation.

(a) If we decide to insulate this tube, what would be the optimum thickness of the insulation?

(b) Show the behavior of heat flow through the tube at different insulation thicknesses such as 0, 3, 6, 10, 15, and 20 mm, and plot the results for $\dot{Q}/L$ versus radius $r$. Assume an insulation material with thermal conductivity $k = 0.06$ W/m K.

*Solution:*

(a) In thermal analysis of radial systems, we must keep in mind that there are competing effects associated with changing the thickness of insulation. Increasing the insulation thickness increases the conduction resistance; however, the area available for convection heat transfer increases as well, resulting in reduced convection resistance. To find the optimum radius for insulation, we first identify the major resistances in the path of heat flow. Our assumptions are that (1) the tube wall thickness is small enough that conduction resistance can be ignored, (2) heat transfer occurs at steady state, (3) insulation has uniform properties, and (4) radial heat transfer is one-dimensional

The resistances per unit length are

$$R_1 = \frac{\ln(r/r_i)}{2\pi k} \quad \text{and} \quad R_2 = \frac{1}{2\pi r h_o},$$

where $r$, the outer radius of insulation, is unknown. The total resistance is

$$R_t = R_1 + R_2 = \frac{\ln(r/r_i)}{2\pi k} + \frac{1}{2\pi r h_o}$$

and the rate of heat flow per unit length is
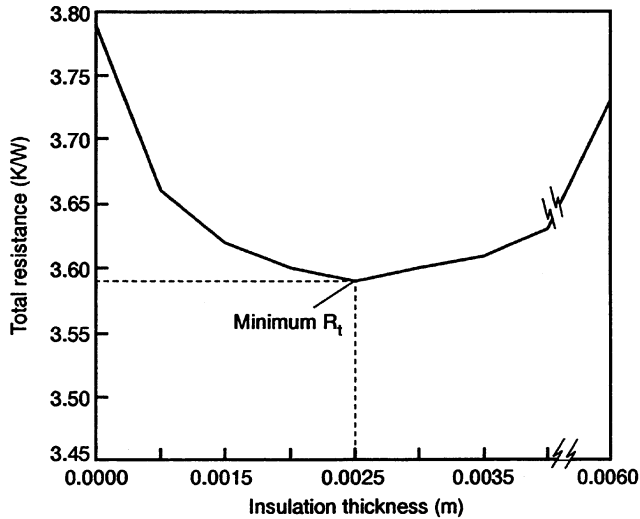
$$\dot{Q} = \frac{T_\infty - T_i}{R_t}.$$

**FIGURE 2.1.16**  Total resistance versus insulation thickness for an insulated tube.

The optimum thickness of the insulation is obtained when the total heat flow is minimized or when the total resistance is maximized. By differentiating $R_t$ with respect to $r$, we obtain the condition under which $R_t$ is maximum (or minimum). Therefore,

$$\frac{dR_t}{dr} = \frac{1}{2\pi r k} - \frac{1}{2\pi r^2 h_o} = 0,$$

from which we obtain $r = k/h_o$. To determine if $R_t$ is maximum or minimum at $r = k/h_o$, we take the second derivative and find its quantity at $r = k/h_o$.

$$\frac{d^2 R_t}{dr^2} = -\frac{1}{2\pi k \left(k/h_o\right)^2} + \frac{1}{\pi h_o \left(k/h_o\right)^3} = \frac{1}{2\pi k^3 / h_o^2} > 0.$$

Therefore, $R_t$ is a *minimum* at $r = k/h_o$, which means that the heat flow is maximum at this insulation radius. An optimum radius of insulation does not exist; however, the radius obtained in this analysis is referred to as the **critical radius**, $r_c$, and this radius should be avoided when selecting insulation for pipes. The economic optimum insulation can be found using techniques in Chapter 3.2.

(b) For this example the critical radius is $r_c = k/h_o = 0.06$ W/m K/7 W/m$^2$ K = 0.0086 m = 8.6 mm, and $r_i = 6$ mm, so $r_c > r_i$. This means that by adding insulation, we will increase the heat loss from the tube. Using the expression for $R_t$, we can plot the total resistance versus the insulation thickness as shown in Figure 2.1.16. Note that the minimum total resistance occurs at an insulation thickness of about 0.025 m (corresponding to the $r_c$ calculated earlier). Also note that as the insulation thickness is increased, the conduction resistance increases; however, the convection resistance decreases as listed in Table 2.1.1.

## Convection Heat Transfer

Energy transport (heat transfer) in fluids usually occurs by the motion of fluid particles. In many engineering problems, fluids come into contact with solid surfaces that are at different temperatures than the fluid. The temperature difference and random/bulk motion of the fluid particles result in an energy transport process known as convection heat transfer. Convection heat transfer is more complicated than conduction because the motion of the fluid, as well as the process of energy transport, must be studied

**TABLE 2.1.1**    Effect of Insulation Thickness on Various Thermal Resistances

| Insulation Thickness (m) | Outer Radius, $r$ (m) | Convection Resistance, $R_2$, (K/W) | Conduction Resistance, $R_1$, (K/W) | Total Resistance, $R_t$, (K/W) |
|---|---|---|---|---|
| 0 | 0.0060 | 3.79 | 0 | 3.79 |
| 0.0010 | 0.0070 | 3.25 | 0.41 | 3.66 |
| 0.0015 | 0.0075 | 3.03 | 0.59 | 3.62 |
| 0.0020 | 0.0080 | 2.84 | 0.76 | 3.60 |
| 0.0025 | 0.0085 | 2.67 | 0.92 | 3.59 |
| 0.0030 | 0.0090 | 2.53 | 1.07 | 3.60 |
| 0.0035 | 0.0095 | 2.39 | 1.22 | 3.61 |
| 0.0040 | 0.0100 | 2.27 | 1.36 | 3.63 |
| 0.0060 | 0.0120 | 1.89 | 1.84 | 3.73 |

simultaneously. Convection heat transfer can be created by external forces such as pumps and fans in a process referred to as **forced convection**. In the absence of external forces, the convection process may result from temperature or density gradients inside the fluid; in this case, the convection heat-transfer process is referred to as **natural convection**. We will discuss this type of convection in more detail in the next section. There are other instances where a heat-transfer process consists of both forced and natural convection modes and they are simply called **mixed-convection** processes.

The main unknown in the convection heat-transfer process is the heat-transfer coefficient (see Eq. 2.1.26). Figure 2.1.17 serves to explain the convection heat-transfer process by showing the temperature and velocity profiles for a fluid at temperature $T_\infty$ and bulk velocity $U_\infty$ flowing over a heated surface. As a result of viscous forces interacting between the fluid and the solid surface, a region known as **velocity boundary layer** is developed in the fluid next to the solid surface. In this region the fluid velocity is zero at the surface and increases to the bulk fluid velocity $u_\infty$. Because of the temperature difference between the fluid and the surface, a region known as **temperature boundary layer** also develops next to the surface, where the temperature at the fluid varies from $T_w$ (surface temperature) to $T_\infty$ (bulk fluid temperature). The velocity-boundary-layer thickness $\delta$ and temperature-boundary-layer thickness $\delta_t$ and their variation along the surface are shown in Figure 2.1.17.

Depending on the thermal diffusivity and kinematic viscosity of the fluid, the velocity and temperature boundary layers may be equal or may vary in size. Because of the no-slip condition at the solid surface, the fluid next to the surface is stationary; therefore, the heat transfer at the interface occurs only by conduction.

If the temperature gradient were known at the interface, the heat exchange between the fluid and the solid surface could be calculated from Eq. (2.1.25), where $k$ in this case is the thermal conductivity of the fluid and $dT/dx$ (or $dT/dy$ in reference to Figure 2.1.17) is the temperature gradient at the interface. However, the temperature gradient at the interface depends on the macroscopic and microscopic motion of fluid particles. In other words, the heat transferred from or to the surface depends on the nature of the flow field.
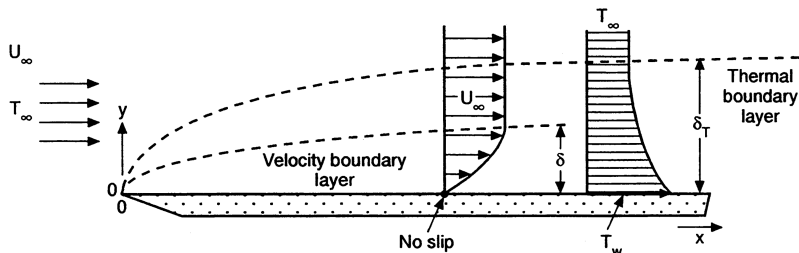


**FIGURE 2.1.17**    Temperature and velocity profiles for convection heat-transfer process over a heated surface.

Therefore, in solving convection problems, engineers need to determine the relationship between the heat transfer through the solid-body boundaries and the temperature difference between the solid-body wall and the bulk fluid. This relationship is given by Eq. (2.1.26), where h is the convection coefficient averaged over the solid surface area. Note that h depends on the surface geometry and the fluid velocity, as well as on the fluid's physical properties. Therefore, depending on the variation of the above quantities, the heat-transfer coefficient may change from one point to another on the surface of the solid body. As a result, the *local* heat-transfer coefficient may be different than the *average* heat-transfer coefficient. However, for most practical applications, engineers are mainly concerned with the *average* heat-transfer coefficient, and in this section we will use only average heat-transfer coefficients unless otherwise stated.

### Natural-Convection Heat Transfer

Natural-convection heat transfer results from density differences within a fluid. These differences may result from temperature gradients that exist within a fluid. When a heated (or cooled) body is placed in a cooled (or heated) fluid, the temperature difference between the fluid and the body causes heat flow between them, resulting in a density gradient inside the fluid. As a result of this density gradient, the low-density fluid moves up and the high-density fluid moves down. The heat-transfer coefficients (and consequently, the rate of heat transfer in natural convection) are generally less than that in forced convection because the driving force for mixing of the fluid is less in natural convection.

Natural-convection problems can be divided into two categories: **external natural convection** and **internal natural convection**. Natural-convection heat transfer from the external surfaces of bodies of various shapes has been studied by many researchers. Experimental results for natural-convection heat transfer are usually correlated by an equation of the type

$$\mathrm{Nu} = \frac{hL}{k} = f\,(\mathrm{Ra}), \qquad (2.1.33)$$

where the **Nusselt number**, Nu, provides a measure of the convection heat transfer occurring between the solid surface and the fluid. Knowing Nu, the convection heat-transfer coefficient, $h$, can be calculated. Note that in Eq. (2.1.33), $k$ is the fluid conductivity and Ra is the **Rayleigh number**, which represents the ratio of buoyancy force to the rate of change of momentum. The Rayleigh number is given by

$$\mathrm{Ra} = \frac{g\beta(T - T_\infty)L^3}{\nu\alpha}, \qquad (2.1.34)$$

where $\beta$ is the coefficient of thermal expansion equal to $1/T$ ($T$ is the absolute temperature expressed in Kelvin) for an ideal gas, L is a characteristic length, $\nu$ is the kinematic viscosity of the fluid, and $\alpha$ is its thermal diffusivity. A comprehensive review of the fundamentals of natural-convection heat transfer is provided by Raithby and Hollands [1985]. Table 2.1.2 gives correlations for calculating heat transfer from the external surfaces of some common geometries.

Experiments conducted by Hassani and Hollands [1989], Sparrow and Stretton [1985], Yovanovich and Jafarpur [1993], and others have shown that the external natural-convection heat transfer from bodies of arbitrary shape exhibit Nu-Ra relationships similar to regular geometries such as spheres and short cylinders. An extensive correlation for predicting natural-convection heat transfer from bodies of arbitrary shape was developed by Hassani and Hollands [1989]; it is useful for most situations on the surfaces of buildings.

Internal natural-convection heat transfer occurs in many engineering problems such as heat loss from building walls, electronic equipment, double-glazed windows, and flat-plate solar collectors. Some of the geometries and their corresponding Nusselt numbers are listed in Table 2.1.3. Anderson and Kreith [1987] provide a comprehensive summary of natural-convection processes that occur in various solar thermal systems.

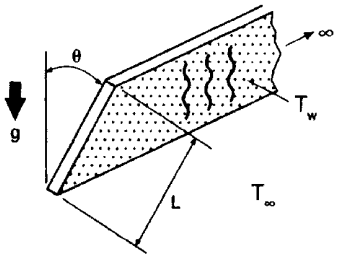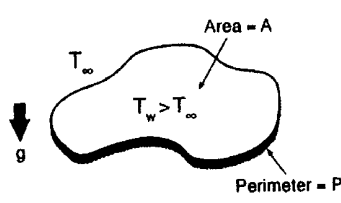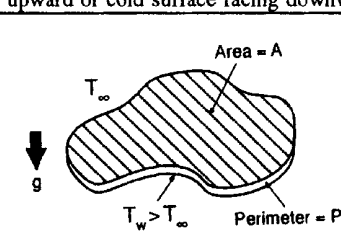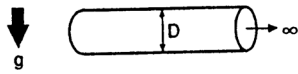**TABLE 2.1.2**   Natural-Convection Correlations for External Flows
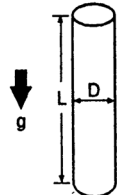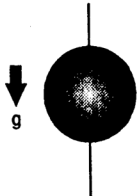
| Configuration | Correlation | Restrictions | Source |
|---|---|---|---|
| <br>Vertical plate with constant $T_w$, $T_\infty$ | $\overline{Nu}_L = \left\{ 0.825 + \dfrac{0.387\ Ra_L^{1/6}}{[1 + (0.492/Pr)^{9/16}]^{8/27}} \right\}^2$ <br><br> $\overline{Nu}_L = 0.56\,(Ra_L \cos\theta)^{1/4}$ | $10^{-1} < Ra_L < 10^{12}$<br>All Pr <br><br> $10^5 < Ra_L \cos\theta < 10^{11}$<br>$0 \le \theta \le 89$ | Churchill and Chu [1975] <br><br><br> Fujii and Imura [1972] |
| <br>Horizontal plate with hot surface facing upward or cold surface facing downward | $\overline{Nu}_L = 0.54\ Ra_L^{1/4}$<br>$\overline{Nu}_L = 0.15\ Ra_L^{1/3}$<br>$\left(L = \dfrac{\text{surface area}}{\text{perimeter}}\right)$ | $10^5 < Ra_L < 10^7$<br>$10^7 < Ra_L < 10^{10}$<br><br>$Pr > 0.5$ | McAdams [1954] and<br>Incropera and DeWitt [1990] |
| <br>Horizontal plate with hot surface facing downward or cold surface facing upward | $\overline{Nu}_L = 0.27\ Ra_L^{1/4}$<br><br><br>$\left(L = \dfrac{\text{surface area}}{\text{perimeter}}\right)$ | $10^5 < Ra_L < 10^{10}$<br><br>$Pr > 0.5$ | McAdams [1954] and<br>Incropera and DeWitt [1990] |

**TABLE 2.1.2 (continued)**  Natural-Convection Correlations for External Flows

| Configuration | Correlation | Restrictions | Source |
|---|---|---|---|
| Horizontal cylinders | $$\overline{Nu}_D = \left\{ 0.6 + \frac{0.387\ Ra_D^{1/6}}{\left[1 + (0.559/Pr)^{9/16}\right]^{8/27}} \right\}^2$$ | $10^{-5} < Ra_D < 10^{12}$<br>All Pr | Churchill and Chu [1975] |
| Vertical cylinders of height L | $$\overline{Nu}_L = 0.68 + \frac{0.67\ Ra_L^{1/4}}{\left[1 + (0.492/Pr)^{9/16}\right]^{4/9}}$$<br><br>$$\overline{Nu}_L = 0.13\ (Ra_L)^{1/3}$$ | $1 < Ra_L < 10^9$<br><br>$\dfrac{D}{L} \ge 35 \left(\dfrac{Pr}{Ra_L}\right)^{1/4}$<br><br>$Ra_L > Pr \times 10^9$ | Churchill and Chu [1975]<br><br>McAdams [1954] |
| Sphere | $$\overline{Nu}_D = 2 + \frac{0.589\ Ra_D^{1/4}}{\left[1 + (0.469/Pr)^{9/16}\right]^{4/9}}$$ | $Pr \ge 0.7$<br>$Ra_D < 10^{11}$ | Churchill [1983] |
| Other immersed bodies such as cubes, bispheres, spheroids | | | Hassani and Hollands [1989] |

*Note*: Ra is Rayleigh number, Pr is Prandtl number, and Nu is Nusselt number.

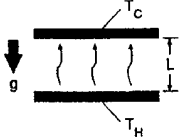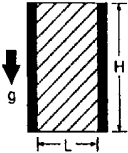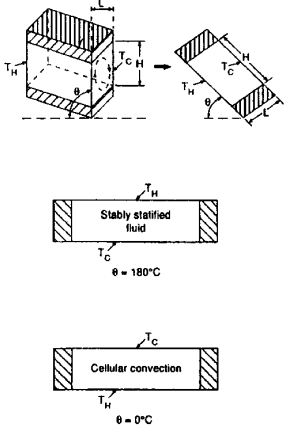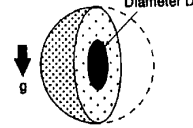**TABLE 2.1.3**  Natural-Convection Correlations for Internal Flows
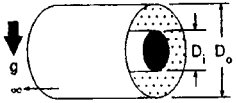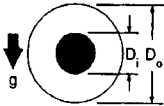
| Configuration | Correlation | Restrictions | Source |
|---|---|---|---|
| Space enclosed between two horizontal plates heated from below | $$\overline{Nu}_L = 1 + 1.44\left[1 - \frac{1708}{Ra_L}\right]^* + \left[\left(\frac{Ra_L}{5830}\right)^{1/3} - 1\right]^*$$ | Air,   $1700 < Ra_L < 10^8$ | Hollands et al. [1975] |
| | $$\overline{Nu}_L = 1 + 1.44\left[1 - \frac{1708}{Ra_L}\right]^* + \left[\left(\frac{Ra_L}{5830}\right)^{1/3} - 1\right]^* + \\ 2.0\left[\frac{Ra_L^{1/3}}{140}\right]^{[1 - \ln(Ra_L^{1/3}/140)]}$$ | Water,   $1700 < Ra_L < 3.5 \times 10^9$ | Hollands et al. [1975] |
| | The quantities contained between the parenthesis with asterisk, ( )$^*$, must be set equal to zero if they become negative. | | |
| Space enclosed between two vertical plates heated from one side | $$\overline{Nu}_L (90°) = 0.22\left(\frac{H}{L}\right)^{-1/4}\left(\frac{Pr}{0.2 + Pr}Ra_L\right)^{0.28}$$ | $2 < \dfrac{H}{L} < 10,$   $Pr < 10,$   $Ra_L < 10^{10}$ | Catton [1978] |
| | $$\overline{Nu}_L (90°) = 0.18\left(\frac{Pr}{0.2 + Pr}Ra_L\right)^{0.29}$$ | $\begin{cases} 1 < \dfrac{H}{L} < 2, \quad 10^{-3} < Pr < 10^5 \\ 10^3 < \dfrac{Ra_L Pr}{0.2 + Pr} \end{cases}$ | |
| | $$\overline{Nu}_L = 0.42\,Ra_L^{0.25}\,Pr^{0.012}\left(\frac{H}{L}\right)^{-0.3}$$ | $\begin{cases} 10 < \dfrac{H}{L} < 40, \quad 1 < Pr < 2 \times 10^4 \\ 10^4 < Ra_L < 10^7 \end{cases}$ | MacGregor and Emery [1969] |

**TABLE 2.1.3 (continued)**   Natural-Convection Correlations for Internal Flows

| Configuration | Correlation | Restrictions | Source |
|---|---|---|---|
| | $\overline{Nu}_L(\theta) = 1 + \left[ Nu_L(90°) - 1 \right] \sin\theta$ | $90° < \theta < 180°$, air | |
| | $\overline{Nu}_L(\theta) = \overline{Nu}_L(90°) (\sin\theta)^{1/4}$ | $\theta^* < \theta < 90$, air | Arnold et al. [1976], Catton (1978), Arnold et al. [1974], and Ayyaswamy and Catton [1973]. Hollands et al. [1976] |
| | $\overline{Nu}_L(\theta) = \left[ \dfrac{\overline{Nu}_L(90°)}{Nu_L(0°)} (\sin\theta^*)^{1/4} \right]^{\theta/\theta^*}$ | $0° < \theta < \theta^*$ , $\dfrac{H}{L} < 10$, air | |
| | $\overline{Nu}_L(\theta) = 1 + 1.44 \left( 1 - \dfrac{1708}{Ra_L \cos\theta} \right)^* \times$ $\left[ 1 - \dfrac{(\sin 1.8\,\theta)^{1.6} \times 1708}{Ra_L \cos\theta} \right] +$ $\left[ \left( \dfrac{Ra_L \cos\theta}{5830} \right)^{1/3} - 1 \right]^*$ | $0° < \theta < \theta^*$ , $\dfrac{H}{L} > 10$, air | |

where

| H/L | 1 | 3 | 6 | 12 | > 12 |
|---|---|---|---|---|---|
| $\theta^*$ | 25° | 53° | 60° | 67° | 70° |

The quantities contained between the parentheses with asterisk, ( )*, must be set equal to zero if they become negative.

Natural convection in inclined enclosures.

---

| Configuration | Correlation | Restrictions | | | Source |
|---|---|---|---|---|---|
| Spherical cavity interior | $\overline{Nu}_D = C(Gr_D Pr)^n$ | $\underline{Gr_D Pr}$ | $\underline{C}$ | $\underline{n}$ | Kreith [1970] |
| | | $10^4$-$10^9$ | 0.59 | 1/4 | |
| | | $10^9$-$10^{12}$ | 0.13 | 1/3 | |

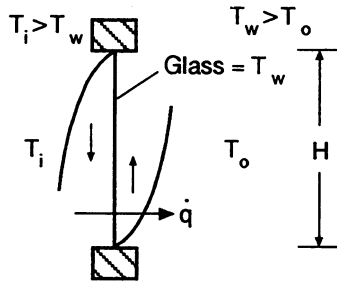| Configuration | Correlation | Restrictions | Source |
|---|---|---|---|
| <br>Long concentric cylinders | $$\frac{k_{eff}}{k} = 0.386 \left[ \frac{\ln(D_o/D_i)}{b^{3/4}(1/D_i^{3/5} + 1/D_o^{3/5})^{5/4}} \right] \times$$ $$\left( \frac{Pr}{0.861 + Pr} \right)^{1/4} Ra_b^{1/4}$$ where $b = (D_o - D_i) / 2$ | $0.70 \leq Pr \leq 6000$ $$10 \leq \left[ \frac{\ln(D_o/D_i)}{b^{3/4}(1/D_i^{3/5} + 1/D_o^{3/5})^{5/4}} \right]^4 Ra_b \leq 10^7$$ | Raithby and Hollands [1974] |
| <br>Concentric spheres | $$\frac{k_{eff}}{k} = 0.74 \left[ \frac{b^{1/4}}{D_o D_i (D_i^{-7/5} + D_o^{-7/5})^{5/4}} \right] \times$$ $$\left( \frac{Pr}{0.861 + Pr} \right)^{1/4} Ra_b^{1/4}$$ where $b = (D_o - D_i) / 2$ | $0.70 \leq Pr \leq 4200$ $$10 \leq \left[ \frac{b}{(D_o D_i)^4 (D_i^{-7/5} + D_o^{-7/5})^5} \right] Ra_b \leq 10^7$$ | Raithby and Hollands [1974] |

**FIGURE 2.1.18**  Heat loss through a single-pane window.

The natural-convection heat transfer for long concentric horizontal cylinders and concentric spheres has been studied by Raithby and Hollands [1985]. Their proposed correlations are listed in Table 2.1.3, where $D_o$ and $D_i$ represent the diameters of outer cylinder (or sphere) and inner cylinder (or sphere), respectively. The Rayleigh number is based on the temperature difference across the gap and a characteristic length defined as $b = (D_o - D_i)/2$. The **effective thermal conductivity** $k_{eff}$ in their correlation is the thermal conductivity that a stationary fluid in the gap must have to transfer the same amount of heat as the moving fluid. Raithby and Hollands also provide correlations for natural-convection heat transfer between long eccentric horizontal cylinders and eccentric spheres.

*Example 2.1.6*

One component of the total heat loss from a room is the heat loss through a single-pane window in the room, as shown in Figure 2.1.18. The inside temperature is kept at $T_i = 22°C$, and the outside temperature is $T_o = -5°C$. The window height $H$ is 0.5 m, and its width is 2 m. The weather is calm, and there is no wind blowing. Assuming uniform glass temperature $T_w$, calculate the heat loss through the window.

*Solution:*

The air flow pattern next to the window is shown in Figure 2.1.18. When warm room air approaches or contacts the window, it loses heat and its temperature drops. Because this cooled air next to the window is denser and heavier than the room air at that height, it starts moving down and is replaced by warmer room air at the top of the window. A similar but opposite air movement occurs at the outside of the window. The total heat loss can be calculated from

$$\dot{Q} = h_i A \left( T_i - T_w \right) = h_o A \left( T_w - T_o \right), \tag{2.1.35}$$

where $h_i$ and $h_o$ are the average natural-convection heat-transfer coefficients for inside and outside, respectively. Using the correlation recommended by Fujii and Imura [1972] for a vertical plate with constant temperature $T_w$ (from Table 2.1.2) and substituting for angle of inclination $\theta = 0$, we get

$$\overline{Nu}_H = 0.56 \ \mathrm{Ra}_H^{1/4},$$

where

$$\mathrm{Ra}_H = \frac{g\beta \ \Delta T \ H^3}{\nu\alpha},$$

and $H$ is the height of the window pane. Note that the temperature difference in the expression for Rayleigh number depends on the medium for which the heat-transfer coefficient is sought. For example, for calculating the interior surface coefficient $h_i$, we write

$$\overline{\mathrm{Nu}}_{H,i} = \frac{h_i H}{k} = 0.56 \left[\frac{g\beta\left(T_i - T_w\right)H^3}{\nu\alpha}\right]^{1/4}, \tag{2.1.36}$$

and for calculating $h_o$, we write

$$\overline{\mathrm{Nu}}_{H,o} = \frac{h_o H}{k} = 0.56 \left[\frac{g\beta\left(T_w - T_o\right)H^3}{\nu\alpha}\right]^{1/4}. \tag{2.1.37}$$

Note that all the properties in Eqs. (2.1.36) or (2.1.37) should be calculated *at film temperature* $T_f = (T_i + T_w)/2$ or $T_f = (T_o + T_w)/2$. To calculate $\dot{Q}$ and air properties, we need to know $T_w$. To estimate $T_w$, we assume that air properties over the temperature range of interest to this problem do not change significantly (refer to air property tables to verify this assumption). Using this assumption, we find the ratio between Eqs. (2.1.36) and (2.1.37) as

$$\frac{h_o}{h_i} = \left(\frac{T_w - T_o}{T_i - T_w}\right)^{1/4}, \tag{2.1.38}$$

which provides a relationship between $h_o$, $h_i$, and $T_w$. Another equation of this kind can be obtained from Eq. (2.1.35):

$$\frac{h_o}{h_i} = \frac{T_i - T_w}{T_w - T_o}. \tag{2.1.39}$$

Solving Eqs. (2.1.38) and (2.1.39), we can show that

$$T_w = \frac{T_o + T_i}{2} = 8.5°\mathrm{C}.$$

Now, by calculating $h_i$ or $h_o$ and substituting into Eq. (2.1.35), the total heat transfer can be calculated. In this case, we choose to solve for $h_o$. Therefore, the air properties should be calculated at

$$T_f = \frac{T_o + T_w}{2} = 1.75°\mathrm{C}.$$

Air properties at $T_f = 1.75°\mathrm{C}$ are $k = 0.0238$ W/m K, $\nu = 14.08 \times 10^{-6}$ m²/s, $\alpha = 19.48 \times 10^{-6}$ m²/s, and $\beta = 1/T_f = 0.00364$ K⁻¹. Using these properties, the Rayleigh number is

$$\mathrm{Ra}_{H,o} = \frac{g\beta\left(T_w - T_o\right)H^3}{\nu\alpha} = 220 \times 10^6.$$

From Eq. (2.1.37), we obtain

$$h_o = \frac{k}{H}\left(0.56\right)\mathrm{Ra}_{H,o}^{1/4} = 3.25 \ \mathrm{W/m^2 \ K},$$

and

$$\dot{Q} = h_o A\left(T_w - T_o\right)$$
$$= 3.25 \ \mathrm{W/m^2 \ K} \times 1 \ \mathrm{m^2} \times \left(281.65 \ \mathrm{K} - 268.15 \ \mathrm{K}\right) = 43.87 \ \mathrm{W}.$$
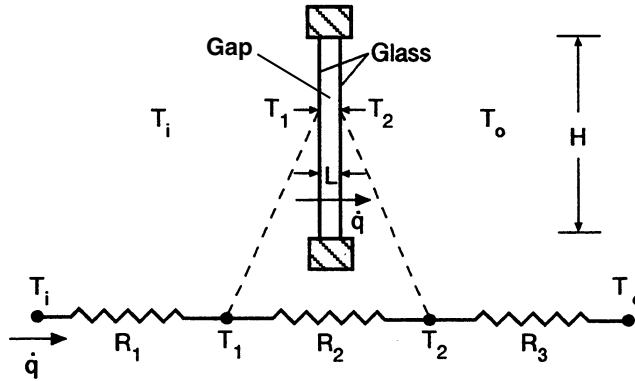
**FIGURE 2.1.19** Heat loss through a double-pane window.

*Example 2.1.7*

The single-pane window of the previous example is replaced by a double-pane window as shown in Figure 2.1.19. The outside and inside temperatures are the same as in Example 2.1.6 ($T_i = 22°C$, $T_o = -5°C$). The glass-to-glass spacing is L = 20 mm, the window height $H = 0.5$ m, and the width is 2 m. Find the heat loss through this window and compare it to the heat loss through the single-pane window. Ignore conduction resistance through the glass.

*Solution:*

The thermal circuit for the system is shown in Figure 2.1.19. Temperatures $T_1$ and $T_2$ are unknown and represent the average glass temperature (i.e., we assume that the glass temperature is uniform over the entire surface because of the low thermal resistance of glass). As in Example 2.1.6, we first estimate temperatures $T_1$ and $T_2$. The rate of heat transfer is

$$\dot{Q} = h_1 A(T_i - T_1) = h_2 A(T_1 - T_2) = h_3 A(T_2 - T_o). \tag{2.1.40}$$

The heat-transfer coefficients $h_1$ and $h_3$ for natural-convection heat transfer between the glass surface and interior/exterior can be calculated using Eqs. (2.1.36) and (2.1.37), and the ratio between $h_1$ and $h_3$ is

$$\frac{h_1}{h_3} = \left(\frac{T_i - T_1}{T_2 - T_o}\right)^{1/4}. \tag{2.1.41}$$

Another relationship between $h_1$, $h_3$, $T_1$, and $T_2$, is obtained from Eq. (2.1.40):

$$\frac{h_1}{h_3} = \left(\frac{T_2 - T_o}{T_i - T_1}\right). \tag{2.1.42}$$

Solving Eqs. (2.1.41) and (2.1.42), we get:

$$T_1 + T_2 = T_i + T_o. \tag{2.1.43}$$

We need an additional equation that provides a relationship between $T_1$ and $T_2$, and we obtain this equation from the correlation that expresses the natural-convection heat transfer in the enclosed area of the double-pane window. We choose the correlation recommended by MacGregor and Emery [1969] from Table 2.1.3:

$$h_2 = \frac{k}{L} \ 0.42 \ \text{Ra}_L^{0.25} \left( \frac{H}{L} \right)^{-0.3} \quad \text{for Pr} = 0.72, \tag{2.1.44}$$

where

$$\text{Ra}_L = \frac{g\beta(T_1 - T_2)L^3}{\nu\alpha}.$$

Using some mathematical manipulations Eq. (2.1.44) can be written as

$$h_2 = \frac{k}{L} 0.16 \left( \frac{T_1 - T_2}{T_i - T_o} \right)^{1/4} \left( \frac{L}{H} \right)^{3/4} \left( \frac{g\beta(T_i - T_o)H^3}{\nu\alpha} \right)^{1/4}, \tag{2.1.45}$$

where $L/H = 0.04$. The heat-transfer coefficient $h_1$ can be calculated from Eq. (2.1.36) (used to calculate $h_i$) and can be written as

$$h_1 = \frac{k}{L} 0.56 \left( \frac{T_i - T_2}{T_i - T_o} \right)^{1/4} \left( \frac{g\beta(T_i - T_o)H^3}{\nu\alpha} \right)^{1/4}, \tag{2.1.46}$$

where the Rayleigh number has been written in terms of $(T_i - T_o)$ instead of $(T_i - T_1)$. Substituting for $L/H$, the ratio between $h_2$ and $h_1$ is

$$\frac{h_2}{h_1} = \frac{0.63 \ (T_1 - T_2)^{1/4}}{(T_i - T_1)^{1/4}}. \tag{2.1.47}$$

Note that in finding $h_2/h_1$, we have assumed that the properties do not change much in the temperature range of interest. From Eq. (2.1.40), we have

$$\frac{h_2}{h_1} = \frac{T_i - T_1}{T_1 - T_2}. \tag{2.1.48}$$

Therefore, solving Eqs. (2.1.47) and (2.1.48), we obtain $T_1$ in terms of $T_i$ and $T_o$:

$$T_1 = 0.71 \ T_i + 0.29 \ T_o. \tag{2.1.49}$$

Substituting for $T_i$ and $T_o$, we obtain $T_1 = 14.2°C$, and substituting for $T_1$, $T_i$, and $T_o$ in Eq. (2.1.43), we get $T_2 = 2.8°C$. Knowing $T_1$ and $T_2$, we can calculate $\text{Ra}_L$. To calculate $\text{Ra}_L$, we should obtain air properties at $T_f = (T_1 + T_2)/2 = 8.5°C$, which are $k = 0.0244$ W/m K, $\nu = 14.8 \times 10^{-6}$ m²/s, $\alpha = 20.6 \times 10^{-6}$ m²/s, and $\beta = 1/T_f = 0.00355$ K⁻¹. Therefore,

$$\text{Ra}_L = \frac{9.81 \ \text{m}/\text{s}^2 \times 0.00355 \ \text{K}^{-1} \times (287.35 \ \text{K} - 275.95 \ \text{K}) \times (0.02)^3 \ \text{m}^3}{14.8 \times 10^{-6} \ \text{m}^2/\text{s} \times 20.6 \times 10^{-6} \ \text{m}^2/\text{s}} = 10,420$$

$h_2$ from Eq. (2.1.44) is

$$h_2 = 1.97 \ \text{W}/\text{m}^2 \ \text{K},$$

and

$$\dot{Q} = h_2 \ A \ (T_1 - T_2) = 22.46 \ \text{W}.$$

Comparing the heat loss to that of Example 2.1.6 for a single-pane window, we note that the heat loss through a single-pane window is almost twice as much as through a double-pane window for the same inside and outside conditions.

**Forced-Convection Heat Transfer**

Forced-convection heat transfer is created by auxiliary means such as pumps and fans or natural phenomena such as wind. This type of process occurs in many engineering applications such as flow of hot or cold fluids inside ducts and various thermodynamic cycles used for refrigeration, power generation, and heating or cooling of buildings. As with natural convection, the main challenge in solving forced-convection problems is to determine the heat-transfer coefficient.

The forced-convection heat transfer processes can be divided into two categories: **external-flow forced convection** and **internal-flow forced convection**. External forced-convection problems are important because they occur in various engineering applications such as heat loss from external walls of buildings on a windy day, from steam radiators, from aircraft wings, or from a hot wire anemometer. To solve these problems, researchers have conducted many experiments to develop correlations for predicting the heat transfer. The experimental results obtained for external forced-convection problems are usually expressed or correlated by an equation of the form

$$\text{Nu} = f(\text{Re}) \ g(\text{Pr}),$$

where $f$ and $g$ represent the functional dependance of the Nusselt number on the Reynolds and Prandtl numbers. The Reynolds number is a nondimensional number representing the ratio of inertia to viscous forces, and the **Prandtl number** is equal to $\nu/\alpha$, which is the ratio of momentum diffusivity to thermal diffusivity.

Table 2.1.4a lists some of the important correlations for calculating forced-convection heat transfer from external surfaces of common geometries. Listed in Table 2.1.4a is the correlation for the forced-convection heat-transfer to or from a fluid flowing over a bundle of tubes, which is relevant to many industrial applications such as the design of commercial heat exchangers. Figures 2.1.20 and 2.1.21 show different configurations of tube bundles in cross-flow whose forced-convection correlations are presented in Table 2.1.4a.

Forced-convection heat transfer in confined spaces is also of interest and has many engineering applications. Flow of cold or hot fluids through conduits and heat transfer associated with that process is important in many HVAC engineering processes. The heat transfer associated with internal forced convection can be expressed by an equation of the form

$$\text{Nu} = f(\text{Re}) \ g(\text{Pr}) \ e(x/D_H),$$

where $f(\text{Re})$, $g(\text{Pr})$, and $e(x/D_H)$ represent the functional dependance on Reynolds number, Prandtl number, and $x/D_H$, respectively. The functional dependance on $x/D_H$ becomes important for short ducts in laminar flow. The quantity $D_H$ is called the **hydraulic diameter** of the conduit and is defined as

$$D_H = 4 \times \frac{\text{flow cross-sectional area}}{\text{wetted perimeter}} \tag{2.1.50}$$

and is used as the characteristic length for Nusselt and Reynolds numbers.

Fully developed laminar flow through ducts of various cross-section has been studied by Shah and London [1978], and they present analytical solutions for calculating heat transfer and friction coefficients.

**TABLE 2.1.4(a)**   Forced-Convection Heat-Transfer Correlations for External Flows*
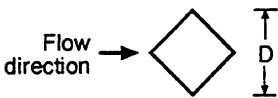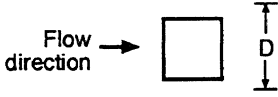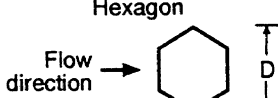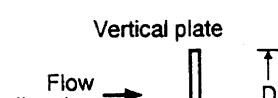
| Configuration | Correlation | Restrictions | Source |
|---|---|---|---|
| Flat plate in parallel flow | $\overline{Nu}_x = 0.664\ Re_x^{1/2}\ Pr^{1/3}$ | Laminar  $Pr \geq 0.6$ | Incropera and DeWitt [1990] |
| Flat plate in parallel flow | $Nu_x = 0.0296\ Re_x^{4/5}\ Pr^{1/3}$ | Turbulent, local,  $0.6 < Pr < 60$, $Re_x < 10^8$ | Incropera and DeWitt [1990] |
| Circular cylinder in cross flow | $\overline{Nu}_D = C\ Re_D^m\ Pr^n\left(\dfrac{Pr_\infty}{Pr_s}\right)^{1/4}$ <br> $n=0.36$ for $Pr > 10$ <br> $n=0.37$ for $Pr \leq 10$ <br><br> $\begin{array}{ccc} \underline{Re_D} & \underline{C} & \underline{m} \\ 1\text{--}40 & 0.75 & 0.4 \\ 40\text{--}1000 & 0.51 & 0.5 \\ 10^3\text{--}2\times10^5 & 0.26 & 0.6 \\ 2\times10^5\text{--}10^6 & 0.076 & 0.7 \end{array}$ | $0.7 < Pr < 500$ <br> $1 < Re_D < 10^6$ <br> Properties at $T_\infty$ | Zukauskas [1972] |
| Non-circular cylinder in cross flow in a gas | $\overline{Nu}_D = C\ Re_D^m\ Pr^{1/3}$ <br><br> For C and m, see Table 4b. | $0.4 < Re_D < 4 \times 10^5$ <br> $Pr \geq 0.7$ | Jakob [1949] |
| Short cylinder in a gas | $\overline{Nu}_D = 0.123\ Re_D^{0.651} + 0.00416\left(\dfrac{D}{L}\right)^{0.85} Re_D^{0.792}$ | $7 \times 10^4 < Re_D < 2.2\times10^5$ <br> $L/D < 4$ | Quarmby and Al-Fakhri [1980] |

**TABLE 2.1.4(a) (continued)    Forced-Convection Heat-Transfer Correlations for External Flows***
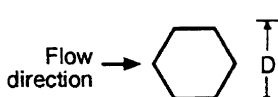
| Configuration | Correlation | Restrictions | Source |
|---|---|---|---|
| Sphere in a gas or liquid | $\overline{Nu}_D = 2 + \left(0.4\ Re_D^{1/2} + 0.06\ Re_D^{2/3}\right) Pr^{0.4} \left(\dfrac{\mu_\infty}{\mu_s}\right)^{1/4}$ | $3.5 < Re_D < 7.6 \times 10^4$ <br> $0.7 < Pr < 380$ <br><br> $1.0 < \dfrac{\mu_\infty}{\mu_s} < 3.2$ <br><br> Properties at $T_\infty$ | Whitaker [1972] |
| Tube bundle in cross-flow | $\overline{Nu}_D = Pr^{+0.36} \left(\dfrac{Pr}{Pr_s}\right)^{1/4} C \left(\dfrac{S_T}{S_L}\right)^n Re_D^m$ <br><br> $\underline{C}\quad\ \underline{m}\quad\ \underline{n}$ <br> $0.8\quad\ 0.4\quad\ 0\qquad 10 < Re_D < 100,\ \text{in-line}$ <br> $0.9\quad\ 0.4\quad\ 0\qquad 10 < Re_D\ 100,\ \text{staggered}$ <br> $0.27\quad 0.63\quad 0\qquad 1000 < Re_D < 2 \times 10^5,\ \text{in-line}$ <br> $\qquad\qquad\qquad\qquad S_T/S_L \geq 0.7$ <br> $0.35\quad 0.60\quad 0.2\quad 1000 < Re_D < 2 \times 10^5,$ <br> $\qquad\qquad\qquad\qquad \text{staggered } S_T/S_L < 2$ <br> $0.40\quad 0.60\quad 0\qquad 1000 < Re_D < 2 \times 10^5,$ <br> $\qquad\qquad\qquad\qquad \text{staggered } S_T/S_L \geq 2$ <br> $0.021\ 0.84\quad 0\qquad Re_D > 2 \times 10^5,\ \text{in-line}$ <br> $0.022\ 0.84\quad 0\qquad Re_D > 2 \times 10^5,\ \text{staggered}$ <br> $\qquad\qquad\qquad\qquad Pr > 1$ <br><br> $\overline{Nu}_D = 0.019\ Re_D^{0.84}\qquad Re_D > 2 \times 10^5,\ \text{staggered}$ <br> $\qquad\qquad\qquad\qquad\qquad Pr = 0.7$ | See Figures 20 and 21 <br><br> Properties at $T_\infty$ | Zukauskas [1972] |
| Flow over staggered tube bundle, gas and liquid | $\overline{Nu}_D = 0.0131\ Re_D^{0.883}\ Pr^{0.36}$ | $4.5 \times 10^5 < Re_D < 7 \times 10^6$ <br> $Pr > 0.5$ <br> $S_T/D = 2,\quad S_L/D = 1.4$ | Achenbach [1989] |

* All properties calculated at $(T_\infty + T_s)/2$ unless otherwise stated under the column "condition." Properties with the subscript "s" are calculated at $T_s$ (surface temperature).

**TABLE 2.1.4(b)**    Constants for Noncircular Cylinders in Cross Flow of a Gas

| Configuration | $Re_D$ | C | m |
|---|---|---|---|
| **Square** | | | |
| Flow direction → ◇ D | $5 \times 10^3 - 10^5$ | 0.246 | 0.588 |
| Flow direction → ☐ D | $5 \times 10^3 - 10^5$ | 0.102 | 0.675 |
| **Hexagon** | | | |
| Flow direction → ⬡ D | $5 \times 10^3 - 1.95 \times 10^4$ $1.95 \times 10^4 - 10^5$ | 0.160 0.0385 | 0.638 0.782 |
| Flow direction → ⬡ D | $5 \times 10^3 - 10^5$ | 0.153 | 0.638 |
| **Vertical plate** | | | |
| Flow direction → ▯ D | $4 \times 10^3 - 1.5 \times 10^4$ | 0.228 | 0.731 |
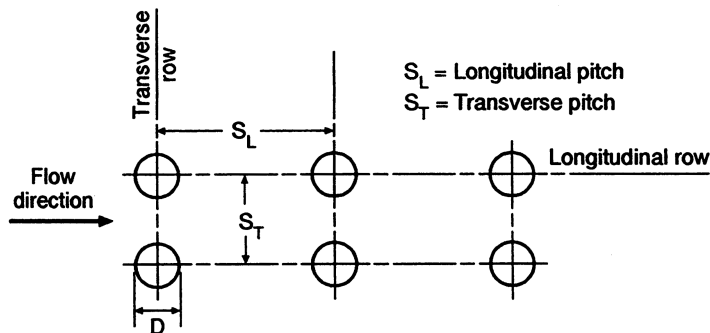


**FIGURE 2.1.20**    In-line tube arrangement for tube bundle in cross-flow forced convection.

Solving internal tube-flow problems requires knowledge of the nature of the tube-surface thermal conditions. Two special cases of tube-surface conditions cover most engineering applications: constant tube-surface heat flux and constant tube-surface temperature. The axial temperature variations for the fluid flowing inside a tube are shown in Figure 2.1.22. Figure 2.1.22(a) shows the mean fluid-temperature variations inside a tube with constant surface heat flux. Note that the mean fluid temperature, $T_m(x)$, varies linearly along the tube. Figure 2.1.22(b) shows the mean fluid-temperature variations inside a tube with constant surface temperature. Some of the recommended correlations for forced convection of incompressible flow inside tubes and ducts are listed in Table 2.1.5.
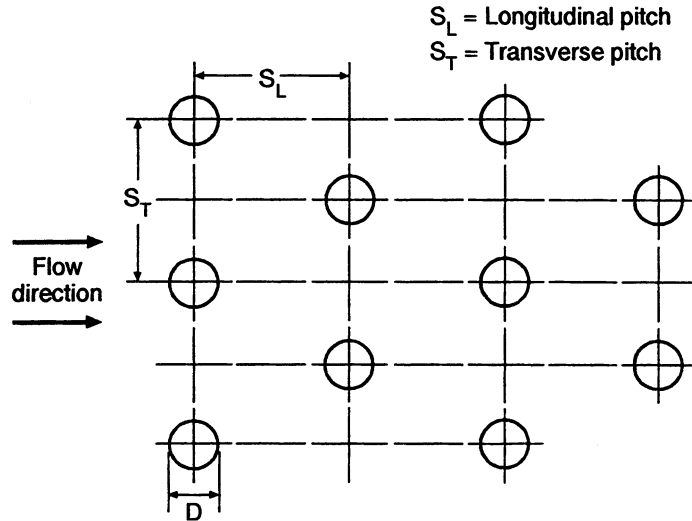
**FIGURE 2.1.21**  Staggered tube arrangement for tube bundle in cross-flow forced convection.
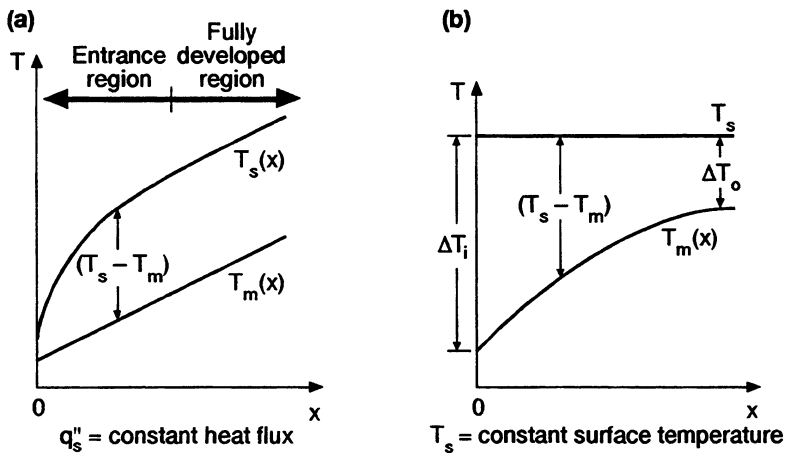


**FIGURE 2.1.22**  Axial fluid temperature variations for heat transfer in a tube for (a) constant surface heat flux, and (b) constant surface temperature.

Now that we have reviewed both natural- and forced-convection heat-transfer processes, it is useful to compare the order of magnitude of the heat-transfer coefficient for both cases. Table 2.1.6 provides some approximate values of convection heat-transfer coefficients.

*Example 2.1.8*

A solar-thermal power plant is depicted in Figure 2.1.23. In this system, solar radiation is reflected from tracking mirrors onto a stationary receiver. The receiver consists of a collection of tubes that are radiatively heated, and a working fluid (coolant) flows through them; the heat absorbed by the working fluid is then used to generate electricity. Consider a central-receiver system that consists of several horizontal circular tubes each with an inside diameter of 0.015 m. The working fluid is molten salt that enters the tube at 400°C at a rate of 0.015 kg/s. Assume that the average solar flux approaching the tube is about 10,000 $W/m^2$.

**TABLE 2.1.5**   Forced-Convection Correlations for Incompressible Flow Inside Tubes and Ducts[*,†]

| Configuration | Correlation | Restrictions | Source |
|---|---|---|---|
| Fully developed laminar flow in long tubes: | | | |
| a. With uniform wall temperature | $\overline{\mathrm{Nu}}_D = 3.66$ | $\mathrm{Pr} > 0.6$ | Kays and Perkins [1985] |
| b. With uniform heat flux | $\overline{\mathrm{Nu}}_D = 4.36$ | $\mathrm{Pr} > 0.6$ | Incropera and DeWitt [1990] |
| c. Friction factor (liquids) | $f = \left(\dfrac{64}{\mathrm{Re}_D}\right)\left(\dfrac{\mu_s}{\mu_b}\right)^{0.14}$ | | |
| d. Friction factor (gas) | $f = \left(\dfrac{64}{\mathrm{Re}_D}\right)\left(\dfrac{T_s}{T_b}\right)^{0.14}$ | | |
| Laminar flow in short tubes and ducts with uniform wall temperature | $\overline{\mathrm{Nu}}_{D_H} = 3.66 + \dfrac{0.0668\ \mathrm{Re}_{D_H}\ \mathrm{Pr}\,\dfrac{D_H}{L}}{1 + 0.045\left(\mathrm{Re}_{D_H}\ \mathrm{Pr}\,\dfrac{D_H}{L}\right)^{0.66}}\left(\dfrac{\mu_b}{\mu_s}\right)^{0.14}$ | $100 < \mathrm{Re}_{D_H}\ \mathrm{Pr}\,\dfrac{D_H}{L} < 1500$ <br> $\mathrm{Pr} > 0.7$ | Hausen [1983] |
| Fully developed turbulent flow through smooth, long tubes and ducts: | | | |
| a. Nusselt number | $\overline{\mathrm{Nu}}_{D_H} = 0.027\ \mathrm{Re}_{D_H}^{0.8}\ \mathrm{Pr}^{0.33}\left(\dfrac{\mu_b}{\mu_s}\right)^{0.14}$ | $6 \times 10^3 < \mathrm{Re}_{D_H} < 10^7$ <br> $0.7 < \mathrm{Pr} < 10^4$ <br> $60 < L/D_H$ | Sieder and Tate [1936] |
| b. Friction factor | $f = \dfrac{0.184}{\mathrm{Re}_{D_H}^{0.2}}$ | $10^4 < \mathrm{Re}_{D_H} < 10^6$ | Kays and London [1984] |

[*] All physical properties are evaluated at the bulk temperature $T_b$ except $\mu_s$, which is evaluated at the surface temperature $T_s$.

[†] Incompressible flow correlations apply to gases and vapors when average velocity is less than half the speed of sound (Mach number < 0.5).

**TABLE 2.1.6**  Order of Magnitude of Convective Heat-Transfer Coefficients $h_c$

|  | W/m² K | Btu/h ft²°F |
|---|---|---|
| Air, free convection | 6–30 | 1–5 |
| Superheated steam or air, forced convection | 3–300 | 5–50 |
| Oil, forced convection | 60–1800 | 10–300 |
| Water, forced convection | 300–18,000 | 50–3000 |
| Water, boiling | 3000–60,000 | 500–10,000 |
| Steam, condensing | 6000–120,000 | 1000–20,000 |
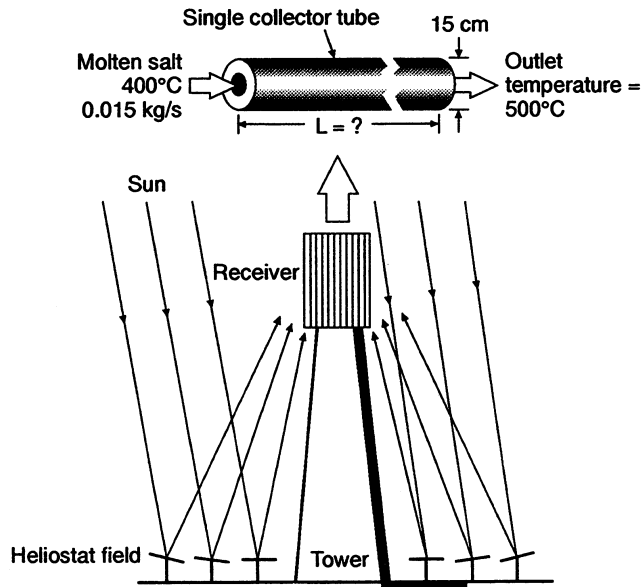


**FIGURE 2.1.23**  A solar-thermal central-receiver system.

(a) Find the necessary length of the tube to raise the working-fluid temperature to 500°C at the exit.

(b) Determine the tube-surface temperature at the exit.

*Solution:*

We will assume steady-state conditions, fully developed flow, and incompressible flow with constant properties. The axial temperature variations for heat transfer in a tube for constant heat flux is shown in Figure 2.1.22(a).

(a) The heat capacity of molten salt at $T_m = (T_i + T_o)/2 = 450°C$ is $c_p = 1{,}520$ J/kg K. The total heat transferred to the working fluid is $q'' A_t = \dot{m}c_p (T_o - T_i)$, where $q''$ is the solar flux and $A_t = \pi D L$ is the surface area of the tube (assuming that the solar flux is incident over the entire perimeter of the tube). Therefore,

$$L = \frac{\dot{m}c_p (T_o - T_i)}{q'' \pi D} = \frac{0.015 \ \text{kg/s} \times 1520 \ \text{J/kg K} \times (773 \ \text{K} - 673 \ \text{K})}{10^4 \ \text{W/m}^2 \times \pi \times 0.015 \ \text{m}} = 4.8 \ m$$

(b) Molten salt properties at $T_o = 500°C$ are $\mu = 1.31 \times 10^{-3}$ Ns/m², $k = 0.538$ W/m K, and Pr = 3.723. The peak tube-surface temperature can be obtained from $q'' = h(T_s - T_o)$, where h is the local convection coefficient at the exit. To find $h$, the nature of the flow must first be established by calculating the Reynolds number:

$$\mathrm{Re} = \frac{uD}{\nu} = \frac{4\dot{m}}{\pi\mu D} = \frac{4 \times 0.015 \ \mathrm{kg/s}}{\pi \times 1.31 \times 10^{-3} \ \mathrm{Ns/m^2} \times 0.015 \ \mathrm{m}} = 972.$$

Because Re < 2,300, the flow inside the tube is laminar. Therefore, from Table 2.1.5, $\mathrm{Nu_D} = hD/k = 4.36$, and

$$h = \frac{\mathrm{Nu}_D k}{D} = \frac{4.36 \times 0.538 \ \mathrm{W/m \ K}}{0.015 \ \mathrm{m}} = 156.4 \ \mathrm{W/m^2 \ K}.$$

The surface temperature at the exit is

$$T_s = \frac{q''}{h} + T_o = \frac{10^4 \ \mathrm{W/m^2}}{156.4 \ \mathrm{W/m^2 \ K}} + 773 \ \mathrm{K} = 836.9 \ \mathrm{K}.$$

### Extended Surfaces or Fins

According to Eq. (2.1.25), the rate of heat transfer by conduction is directly proportional to the heat flow area. To enhance the rate of heat transfer, we can increase the effective heat-transfer surface area. Based on this concept, extended surfaces or fins are widely used in industry to increase the rate of heat transfer for heating or cooling purposes. Various types of extended surfaces are shown in Figure 2.1.24. The simplest type of extended surface is the fin with a uniform cross-section, as shown in Figure 2.1.24(d). The temperature distribution and fin heat-transfer rate can be found by solving a differential equation that expresses energy balance on an infinitesimal element in the fin as given by

$$\frac{d^2T(x)}{dx^2} - \frac{hP}{kA}\left[T(x) - T_\infty\right] = 0, \tag{2.1.51}$$

where $P$ is the cross-sectional perimeter of the fin, $k$ is the thermal conductivity of the fin, $A$ is the cross-sectional area of the fin, and h is the mean convection heat-transfer coefficient between the fin and its surroundings. To solve Eq. (2.1.51), we need two boundary conditions: one at $x = 0$ (base of the fin) and the other at $x = $ L (tip of the fin). The boundary condition used at the base of the fin is usually $T(x = 0) = T_b$, the temperature of the main body to which the fin is attached. The second boundary condition at the tip of the fin ($x = L$) may take several forms:

1. The fin temperature approaches the environment temperature:

$$T \approx T_\infty \quad at \quad x = L.$$

2. There is no heat loss from the end surface of the fin (insulated end):

$$\frac{dT}{dx} = 0 \quad at \quad x = L.$$

3. The fin-end surface temperature is fixed:

$$T = T_L \quad at \quad x = L.$$

4. There is convection heat loss from the end surface of the fin:

$$-k \left.\frac{dT}{dx}\right|_{x=L} = h_L \left(T_L - T_\infty\right).$$
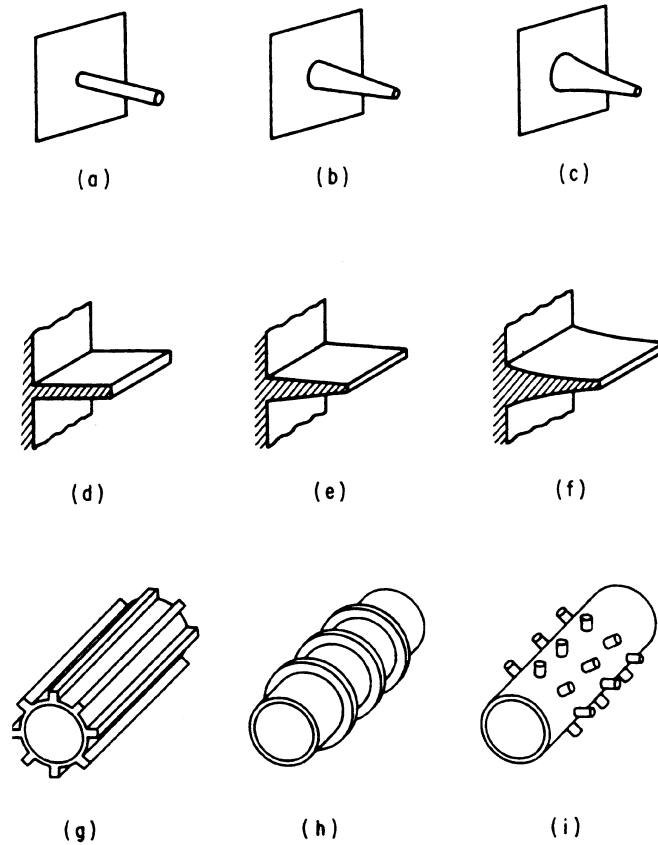
**FIGURE 2.1.24**  Various types of extended surfaces. Designs (d) – (f) are often used in HVAC heating or cooling coils.

Using the boundary condition at $x = 0$ along with one of the four boundary conditions for $x = L$, we can solve Eq. (2.1.51) and obtain the temperature distribution for a fin with a uniform cross section. Knowing the temperature distribution of the fin, the fin heat-transfer rate $q_{fin}$ can be obtained by applying Fourier's law at the base of the fin:

$$-kA \left. \frac{dT}{dx} \right|_{x=0} = -kA \left. \frac{d\theta}{dx} \right|_{x=0}, \tag{2.1.52}$$

where $A$ is the cross-sectional surface area of the fin and $\theta(x) = T(x) - T_\infty$. Figure 2.1.25 is a schematic representation of the temperature distribution in a fin with boundary condition 4. Table 2.1.7 lists equations of temperature distribution and rate of heat transfer for fins of uniform cross section with all four different tip boundary conditions.

Fins or extended surfaces are used to increase the heat-transfer rate from a surface. However, the presence of fins introduces an additional conduction resistance in the path of heat dissipating from the base surface. If a fin is made of highly conductive material, its resistance to heat conduction is small, creating a small temperature gradient from the base to the tip of the fin. However, fins show a temperature distribution similar to that shown in Figure 2.1.25. Therefore, the thermal performance of fins is usually assessed by calculating **fin efficiency**.

The efficiency of a fin is defined as the ratio of the actual heat loss to the maximum heat loss that would have occurred if the total surface of the fin were at the base temperature, that is,

**TABLE 2.1.7**  Equations for Temperature Distribution and Rate of Heat Transfer for Fins of Uniform Cross Section*

| Case | Tip Condition $(x = L)$ | Temperature Distribution $(\theta/\theta_b)$ | Fin Heat-Transfer Rate $(q_{fin})$ |
|---|---|---|---|
| 1 | Infinite fin $(L \to \infty)$: $\theta(L) = 0$ | $e^{-\mu x}$ | $M$ |
| 2 | Adiabatic: $\left.\dfrac{d\theta}{dx}\right|_{x=L} = 0$ | $\dfrac{\cosh m(L-x)}{\cosh mL}$ | $M \tanh mL$ |
| 3 | Fixed temperature: $\theta(L) = \theta_L$ | $\dfrac{(\theta_L/\theta_b)\sinh mx + \sinh m(L-x)}{\sinh mL}$ | $M\,\dfrac{\cosh mL - (\theta_L/\theta_b)}{\sinh mL}$ |
| 4 | Convection heat transfer: $h\theta(L) = k\left.\dfrac{d\theta}{dx}\right|_{x=L}$ | $\dfrac{\cosh m(L-x) + (h/mk)\,\sinh m(L-x)}{\cosh mL + (h/mk)\,\sinh mL}$ | $M\,\dfrac{\sinh mL + (h/mk)\,\cosh mL}{\cosh mL + (h/mk)\,\sinh mL}$ |

* $\theta \equiv T - T_\infty$; $\theta_b \equiv \theta(0) = T_b - T_\infty$; $m^2 \equiv \dfrac{hP}{kA}$; $M \equiv \sqrt{hPkA}\;\theta_b$.
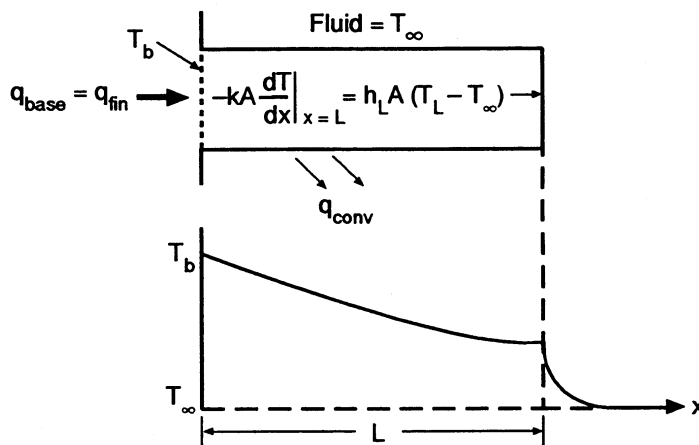


**FIGURE 2.1.25**  Schematic representation of temperature distribution in a fin with boundary condition 4 at its tip.

$$\eta_{fin} = \frac{q_{fin}}{q_{max}} = \frac{q_{fin}}{hA_f(T_b - T_\infty)}, \tag{2.1.53}$$

where $A_f$ is the total surface area of the fin, and $q_{fin}$ for fins with uniform cross section is obtained from Table 2.1.7.

### Radiation Heat Transfer

Thermal radiation is a heat-transfer process that occurs between any two objects that are at different temperatures. All objects emit thermal radiation by virtue of their temperature. Scientists believe that the thermal radiation energy emitted by a surface is propagated through the surrounding medium either by electromagnetic waves or is transported by photons. In a vacuum, radiation travels at the speed of light $C_0$ ($3 \times 10^8$ m/s in a vacuum); however, the **speed of propagation** $c$ in a medium is less than $C_0$ and is given in terms of index of refraction of the medium, as in Eq. (2.1.54). The radiation wavelength depends on the source frequency and refractive index of the medium through which the radiation travels, according to the equation

$$c = \lambda v = \frac{C_0}{n}, \qquad (2.1.54)$$

where  $n$ = index of refraction of the medium

$C_0 = 3 \times 10^8$ m/s ($9.84 \times 10^8$ ft/s)

$\lambda$ = wavelength, m (ft)

$v$ = frequency, $s^{-1}$

Thermal radiation can occur over a wide spectrum of wavelengths, namely between 0.1 and 100 μm. The spectral distribution and the magnitude of the emitted radiation from an object depends strongly on its absolute temperature and the nature of its surface. For example, at the surface temperature of the sun, 5,800 K, most energy is emitted at wavelengths near 0.3 μm. However, thermal processes within buildings occur at 10 μm. This particular radiation-process property has caused environmental concerns such as global warming (or the greenhouse effect) in recent years. Global warming is a result of the increased amount of carbon dioxide in the atmosphere. This gas absorbs radiation from the sun at shorter wavelengths but is opaque to emitted radiation from the earth at longer wavelengths, thereby trapping the thermal energy and causing a gradual warming of the atmosphere, as in a greenhouse.

A perfect radiator—called a **blackbody**—emits and absorbs the maximum amount of radiation at any wavelength. The amount of heat radiated by a blackbody is

$$\dot{Q}_r = \sigma A T_b^4, \qquad (2.1.55)$$

where  $\sigma$ = the Stefan–Boltzmann constant = $5.676 \times 10^{-8}$ W/m$^2$ K$^4$ (or $0.1714 \times 10^{-8}$ Btu/h ft$^2$ °R$^4$)

$T_b$ = absolute temperature of the blackbody, K (°R)

$A$ = surface area, m$^2$ (ft$^2$)

The spectral (or monochromatic) **blackbody emissive power** according to Planck's Law is

$$E_{b\lambda}(T) = \frac{C_1 \lambda^{-5}}{e^{C_2/\lambda T} - 1}, \qquad (2.1.56)$$

where  $E_{b\lambda}(T)$ = spectral emissive power of a blackbody at absolute temperature $T$, $\dfrac{W}{m^3}\left(\dfrac{Btu}{h\,ft^2\mu}\right)$

$\lambda$ = wavelength, m (μ)

$T$ = absolute temperature of blackbody, K (°R)

$C_1$ = constant, $3.7415 \times 10^{-16}$ W m$^2$ $\left(1.187 \times 10^8\,\dfrac{Btu\,\mu^4}{h\,ft^2}\right)$

$C_2$ = constant, $1.4388 \times 10^{-2}$ m K ($2.5896 \times 10^4$ μ °R)

The spectral blackbody emissive power for different temperatures is plotted in Figure 2.1.26, which shows that as the temperature increases, the emissive power and the wavelength range increase as well. However, as temperature increases, the wavelength at which maximum emissive power occurs decreases. Wien's Displacement Law provides a relationship between the maximum power wavelength $\lambda_{max}$ and the absolute temperature at which $E_{b\lambda}$ is maximum:

$$\lambda_{max}\ T = 2.898 \times 10^{-3}\ \text{mK} = 5216.4\ \mu\ °R.$$

To obtain the total emissive power of a blackbody, we integrate the spectral emissive power over all wavelengths:

$$E_b = \int_0^\infty E_{b\lambda}\ d\lambda = \sigma T_b^4. \qquad (2.1.57)$$
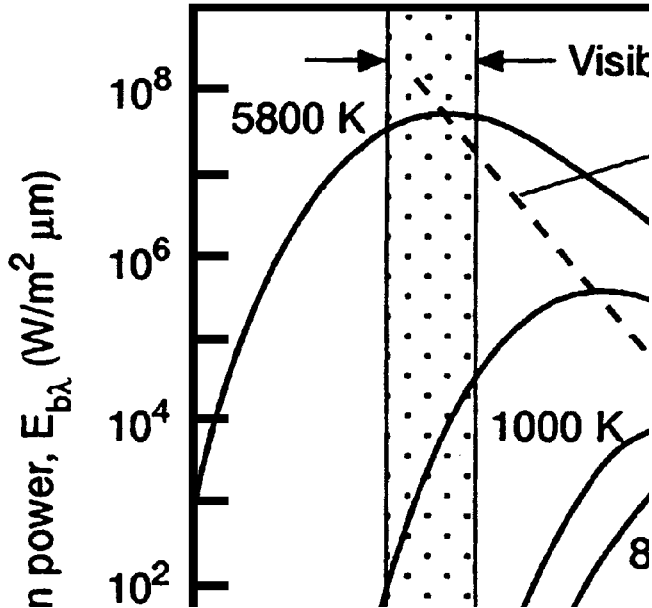
**FIGURE 2.1.26**  Spectral blackbody emissive power for different temperatures.

Equation (2.1.57) is the same as Eq. (2.1.55) except that it is expressed per unit area. At a given temperature $T_b$, the quantity $E_b$ of Eq. (2.1.57) is the area under the curve corresponding to $T_b$ in Figure 2.1.26.

Engineers sometimes encounter problems where it is necessary to find the fraction of the total energy radiated from a blackbody in a finite interval between two specific wavelengths $\lambda_1$ and $\lambda_2$. This fraction for an interval from 0 to $\lambda_1$ can be determined from:

$$B\left(0 \rightarrow \lambda_1\right) = \frac{\displaystyle\int_0^{\lambda_1} E_{b\lambda}\ d\lambda}{\displaystyle\int_0^{\infty} E_{b\lambda}\ d\lambda} = \frac{\displaystyle\int_0^{\lambda_1} E_{b\lambda}\ d\lambda}{\sigma T_b^4}.$$

This integral has been calculated for various $\lambda T$ quantities, and the results are presented in Table 2.1.8. The fraction of total radiation from a blackbody in a finite wavelength interval from $\lambda_1$ to $\lambda_2$ can then be obtained from

$$B\left(\lambda_1 \rightarrow \lambda_2\right) = \frac{\displaystyle\int_0^{\lambda_2} E_{b\lambda}\ d\lambda - \int_0^{\lambda_1} E_{b\lambda}\ d\lambda}{\sigma T_b^4} = B\left(0 \rightarrow \lambda_2\right) - B\left(0 \rightarrow \lambda_1\right)$$

where quantities $B(0 \rightarrow \lambda_2)$ and $B(0 \rightarrow \lambda_1)$ can be read from Table 2.1.8.

### Radiation Properties of Objects

When radiation strikes the surface of an object, a portion of the total incident radiation is reflected, a portion is absorbed, and if the object is transparent, a portion is transmitted through the object, as depicted in Figure 2.1.27.

The fraction of incident radiation which is reflected is called the **reflectance** (**or reflectivity**) $\rho$, the fraction transmitted is called the **transmittance** (**or transmissivity**) $\tau$, and the fraction absorbed is called the

**TABLE 2.1.8**  Blackbody Radiation Functions

| $\lambda T$ $(mK \times 10^3)$ | $B(0 \rightarrow \lambda)$ | $\lambda T$ $(mK \times 10^3)$ | $B(0 \rightarrow \lambda)$ |
|---|---|---|---|
| 0.2 | $0.341796 \times 10^{-26}$ | 6.2 | 0.754187 |
| 0.4 | $0.186468 \times 10^{-11}$ | 6.4 | 0.769234 |
| 0.6 | $0.929299 \times 10^{-7}$ | 6.6 | 0.783248 |
| 0.8 | $0.164351 \times 10^{-4}$ | 6.8 | 0.796180 |
| 1.0 | $0.320780 \times 10^{-3}$ | 7.0 | 0.808160 |
| 1.2 | $0.213431 \times 10^{-2}$ | 7.2 | 0.819270 |
| 1.4 | $0.779084 \times 10^{-2}$ | 7.4 | 0.829580 |
| 1.6 | $0.197204 \times 10^{-1}$ | 7.6 | 0.839157 |
| 1.8 | $0.393499 \times 10^{-1}$ | 7.8 | 0.848060 |
| 2.0 | $0.667347 \times 10^{-1}$ | 8.0 | 0.856344 |
| 2.2 | 0.100897 | 8.5 | 0.856344 |
| 2.4 | 0.140268 | 9.0 | 0.890090 |
| 2.6 | 0.183135 | 9.5 | 0.903147 |
| 2.8 | 0.227908 | 10.0 | 0.914263 |
| 3.0 | 0.273252 | 10.5 | 0.923775 |
| 3.2 | 0.318124 | 11.0 | 0.931956 |
| 3.4 | 0.361760 | 11.5 | 0.939027 |
| 3.6 | 0.403633 | 12 | 0.945167 |
| 3.8 | 0.443411 | 13 | 0.955210 |
| 4.0 | 0.480907 | 14 | 0.962970 |
| 4.2 | 0.516046 | 15 | 0.969056 |
| 4.4 | 0.548830 | 16 | 0.973890 |
| 4.6 | 0.579316 | 18 | 0.980939 |
| 4.8 | 0.607597 | 20 | 0.985683 |
| 5.0 | 0.633786 | 25 | 0.992299 |
| 5.2 | 0.658011 | 30 | 0.995427 |
| 5.4 | 0.680402 | 40 | 0.998057 |
| 5.6 | 0.701090 | 50 | 0.999045 |
| 5.8 | 0.720203 | 75 | 0.999807 |
| 6.0 | 0.737864 | 100 | 1.000000 |
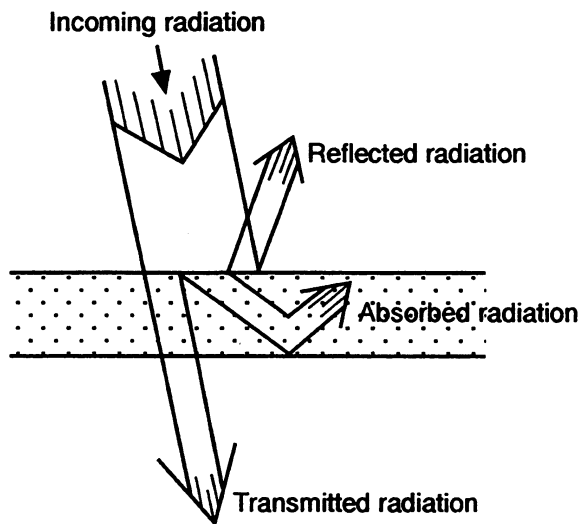


**FIGURE 2.1.27**   Schematic of reflected, transmitted, and absorbed radiation.

**absorptance** (**or absorptivity**) $\alpha$. There are two types of radiation reflections: specular and diffuse. A **specular reflection** is one in which the angle of incidence is equal to the angle of reflection, whereas a **diffuse reflection** is one in which the incident radiation is reflected uniformly in all directions. Highly polished surfaces such as mirrors approach the specular reflection characteristics, but most industrial surfaces (rough surfaces) have diffuse reflection characteristics. By applying an energy balance to the surface of the object as shown in Figure 2.1.27, the relationship between these properties can be expressed as

$$\alpha + \rho + \tau = 1. \tag{2.1.58}$$

The relative magnitude of each one of these components depends on the characteristics of the surface, its temperature, and the spectral distribution of the incident radiation. If an object is opaque ($\tau = 0$), it will not transmit any radiation. Therefore

$$\alpha + \rho = 1 \quad \text{and} \quad \tau = 0 \quad \text{for an opaque object.} \tag{2.1.59}$$

If an object has a perfectly reflecting surface (a good mirror), then it will reflect all the incident radiation, and

$$\rho = 1, \quad \alpha = 0, \quad \text{and} \quad \tau = 0 \quad \text{for a perfectly reflective surface.} \tag{2.1.60}$$

The **emissivity**, $\varepsilon$, of a surface at temperature $T$ is defined as the ratio of total energy emitted to the energy that would be emitted by a blackbody at the same temperature $T$:

$$\varepsilon = \frac{E(T)}{\sigma T^4}, \tag{2.1.61}$$

where $E(T)$ represents the radiation energy emitted from the surface. For a blackbody, Eq. (2.1.61) gives $\varepsilon_b = 1$. The absorptivity for a blackbody is also equal to unity; therefore, $\varepsilon_b = \alpha_b = 1$.

A special type of surface called a gray surface or **graybody** is a surface with spectral emissivity and absorptivity that are both independent of the wavelength. Therefore, for a graybody, $\bar{\alpha} = \alpha_\lambda = \bar{\varepsilon} = \varepsilon_\lambda$ where $\bar{\varepsilon}$ and $\bar{\alpha}$ are the average values of emissivity and absorptivity, respectively. In many engineering problems, surfaces are not gray surfaces. However, one can employ graybody assumptions by using suitable $\bar{\alpha}$ and $\bar{\varepsilon}$ values.

Table 2.1.9 provides emissivities of various surfaces at several wavelengths and temperatures. A more extensive list of experimentally measured radiation properties of various surfaces has been provided by Gubareff et al. [1960] and Kreith and Bohn [1993]; note that the listed quantities in Table 2.1.9 are hemispherical emissivities. Detailed directional and spectral measurements of radiation properties of surfaces are limited in the literature. Because of the difficulties in performing these detailed measurements, most of the tabulated properties are averaged quantities, such as those presented in Table 2.1.9. Properties averaged with respect to wavelength are termed *total* quantities, and properties averaged with respect to direction are termed *hemispherical* quantities. Hemispherical spectral emissivity of a surface is the ratio of (1) the spectral radiation emitted by a unit surface area of an object into all directions of a hemisphere surrounding that area to (2) the spectral radiation emitted by a unit surface area of a blackbody (at the same temperature) into all directions of that hemisphere.

***The Radiation Shape Factor (View Factor)***
In this section, we will only deal with surfaces that have diffuse reflection characteristics, because most real surfaces used in different industries can be assumed to have diffuse reflection characteristics. In solving radiation problems, we must find out how much of the radiation leaving one surface is being intercepted by another surface.

**TABLE 2.1.9**    Hemispherical Emissivities of Various Surfaces[a]

| Material | 9.3 mm 310 K | 5.4 mm 530 K | 3.6 mm 800 K | 1.8 mm 1700 K | 0.6 mm Solar ~6,000 K |
|---|---|---|---|---|---|
| | | | Metals | | |
| **Aluminum** | | | | | |
| polished | ~0.04 | 0.05 | 0.08 | ~0.19 | ~0.30 |
| oxidized | 0.11 | ~0.12 | 0.18 | | |
| 24-ST weathered | 0.40 | 0.32 | 0.27 | | |
| surface roofing | 0.22 | | | | |
| anodized (at 1,000°F) | 0.94 | 0.42 | 0.60 | 0.34 | |
| **Brass** | | | | | |
| polished | 0.10 | 0.10 | | | |
| oxidized | 0.61 | | | | |
| **Chromium** | | | | | |
| polished | ~0.08 | ~0.17 | 0.26 | ~0.40 | 0.49 |
| **Copper** | | | | | |
| polished | 0.04 | 0.05 | ~0.18 | ~0.17 | |
| oxidized | 0.87 | 0.83 | 0.77 | | |
| **Iron** | | | | | |
| polished | 0.06 | 0.08 | 0.13 | 0.25 | 0.45 |
| cast, oxidized | 0.63 | 0.66 | 0.76 | | |
| galvanized, new | 0.23 | | | 0.42 | 0.66 |
| galvanized, dirty | 0.28 | | | 0.90 | 0.89 |
| steel plate, rough | 0.94 | 0.97 | 0.98 | | |
| oxide | 0.96 | | 0.85 | | 0.74 |
| molten | | | | 0.3–0.4 | |
| **Magnesium** | 0.07 | 0.13 | 0.18 | 0.24 | 0.30 |
| **Molybdenum filament** | | | ~0.09 | ~0.15 | ~0.20[b] |
| **Silver** | | | | | |
| polished | 0.01 | 0.02 | 0.03 | | 0.11 |
| **Stainless steel** | | | | | |
| 18-8, polished | 0.15 | 0.18 | 0.22 | | |
| 18-8, weathered | 0.85 | 0.85 | 0.85 | | |
| **Steel tube** | | | | | |
| oxidized | | 0.94 | | | |
| **Tungsten filament** | 0.03 | | | ~0.18 | 0.35[c] |
| **Zinc** | | | | | |
| polished | 0.02 | 0.03 | 0.04 | 0.06 | 0.46 |
| galvanized sheet | ~0.25 | | | | |
| | | Building and Insulating Materials | | | |
| Asbestos paper | 0.93 | 0.93 | | | |
| Asphalt | 0.93 | | 0.90 | | 0.93 |
| **Brick** | | | | | |
| red | 0.93 | | | | 0.70 |
| fire clay | 0.90 | | ~0.70 | ~0.75 | |
| silica | 0.90 | | 0.75 | 0.84 | |
| magnesite refractory | 0.90 | | | ~0.40 | |
| Enamel, white | 0.90 | | | | |
| Marble, white | 0.95 | | 0.93 | | 0.47 |
| Paper, white | 0.95 | | 0.82 | 0.25 | 0.28 |
| Plaster | 0.91 | | | | |
| Roofing board | 0.93 | | | | |
| Enameled steel, white | | | | 0.65 | 0.47 |
| Asbestos cement, red | | | | 0.67 | 0.66 |

**TABLE 2.1.9 (continued)**     Hemispherical Emissivities of Various Surfaces[a]

| | Wavelength and Average Temperature | | | | |
|---|---|---|---|---|---|
| Material | 9.3 mm<br>310 K | 5.4 mm<br>530 K | 3.6 mm<br>800 K | 1.8 mm<br>1700 K | 0.6 mm<br>Solar ~6,000 K |
| | | | Paints | | |
| Aluminized lacquer | 0.65 | 0.65 | | | |
| Cream paints | 0.95 | 0.88 | 0.70 | 0.42 | 0.35 |
| Lacquer, black | 0.96 | 0.98 | | | |
| Lampblack paint | 0.96 | 0.97 | | 0.97 | 0.97 |
| Red paint | 0.96 | | | | 0.74 |
| Yellow paint | 0.95 | | 0.50 | | 0.30 |
| Oil paints (all colors) | ~0.94 | ~0.90 | | | |
| White (ZnO) | 0.95 | | 0.91 | | 0.18 |
| | | | Miscellaneous | | |
| Ice | ~0.97[d] | | | | |
| Water | ~0.96 | | | | |
| Carbon | | | | | |
|   T-carbon, 0.9% ash | 0.82 | 0.80 | 0.79 | | |
|   filament | ~0.72 | | | 0.53 | |
| Wood | ~0.93 | | | | |
| Glass | 0.90 | | | | (Low) |

[a] Since the emissivity at a given wavelength equals the absorptivity at that wavelength, the values in this table can be used to approximate the absorptivity to radiation from a source at the temperature listed. For example, polished aluminum will absorb 30% of incident solar radiation.

[b] At 3,000 K.

[c] At 3,600 K.

[d] At 273 K.

*Sources:* Fischenden and Saunders [1932]; Hamilton and Morgan [1962]; Kreith and Black [1980]; Schmidt and Furthman [1928]; McAdams [1954]; Gubareff et al. [1960].

The **radiation shape** factor $F_{1-2}$ is defined as

$$F_{1-2} = \frac{\text{diffuse radiation leaving surface A}_1 \text{ and being intercepted by surface A}_2}{\text{total diffuse radiation leaving surface A}_1}.$$

For example, consider two black surfaces $A_1$ and $A_2$ at temperatures $T_1$ and $T_2$, as shown in Figure 2.1.28. The radiation leaving surface $A_1$ and reaching $A_2$ is

$$\dot{Q}_{1\rightarrow 2} = A_1 F_{1-2} E_{b1}, \tag{2.1.62}$$

and the radiation leaving surface $A_2$ and reaching surface $A_1$ is

$$\dot{Q}_{2\rightarrow 1} = A_2 F_{2-1} E_{b2}, \tag{2.1.63}$$

From Eqs. (2.1.62) and (2.1.63), we can calculate the net radiation heat exchange between these two black surfaces:

$$\Delta\dot{Q}_{1\rightarrow 2} = A_1 F_{1-2} E_{b1} - A_2 F_{2-1} E_{b2}.$$

Shape factors for some geometries that have engineering applications are presented in Table 2.1.10. For more information and an extensive list of shape factors, refer to Siegel and Howell [1972].
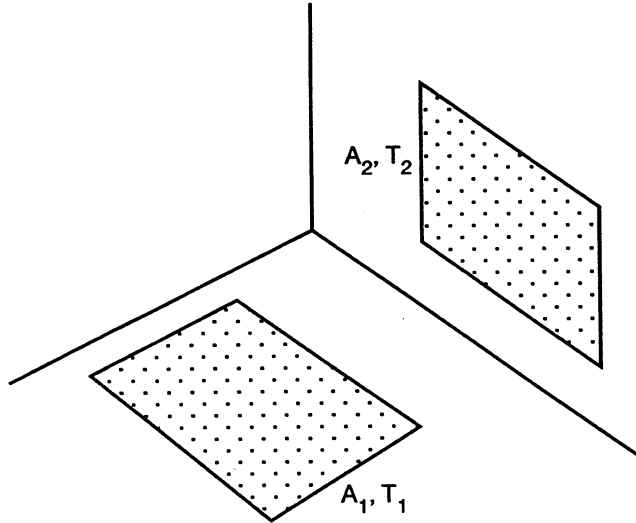
**FIGURE 2.1.28**  Sketch illustrating the nomenclature for shape factor between the two surfaces $A_1$ and $A_2$.

*Example 2.1.9*

A flat-plate solar collector with a single glass cover to be used for building water heating is shown in Figure 2.1.29. The following quantities are known:

The solar irradiation, $G_s = 750$ W/m$^2$
The absorptivity of the cover plate to solar radiation, $\alpha_{cp,s} = 0.16$
The transmissivity of the cover plate to solar radiation, $\tau_{cp} = 0.84$
The emissivity of the cover plate to longwave radiation, $\varepsilon_{cp} = 0.9$
The absorptivity of the absorber plate to solar radiation, $\alpha_{ap,s} = 1.0$
The emissivity of the absorber plate to longwave radiation, $\varepsilon_{ap} = 0.1$
The convection coefficient between the absorber plate and the cover plate, $h_i = 2$ W/m$^2$ K
The convection coefficient between the cover plate and ambient, $h_o = 5$ W/m$^2$ K
The absorber-plate temperature, $T_{ap} = 120°$C
The ambient air temperature $T_\infty = 30°$C
The effective sky temperature, $T_{sky} = -10°$C

Using this information, calculate the useful heat absorbed by the absorber plate.

*Solution:*

We will assume the following:

- Steady-state conditions
- Uniform surface heat-flux and temperature for the cover plate and the absorber plate
- Opaque, diffuse-gray surface behavior for longwave radiation
- Well-insulated absorber plate

To find the useful heat absorbed by the absorber plate, perform an energy balance on a unit area of the absorber plate, as in Figure 2.1.30:

$$\alpha_{ap,s}\ \tau_{cp,s}\ G_s = q_{conv,i} + q_{rad,ap-cp} + q_u, \tag{2.1.64}$$
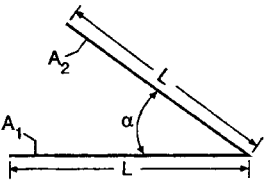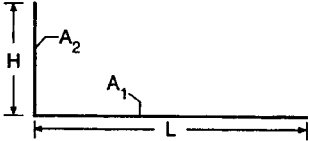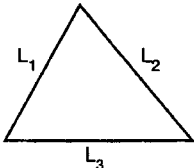
**TABLE 2.1.10**  Minicatalog of Geometric View Factors
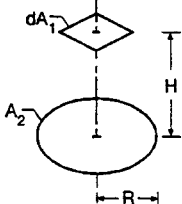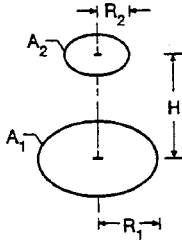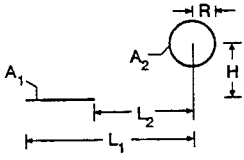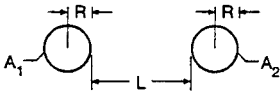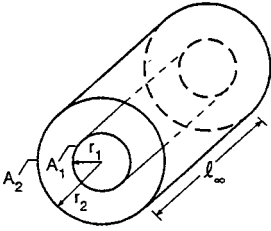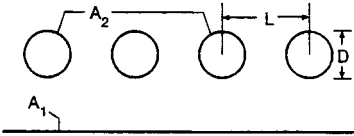
| Configuration | Geometric View Factor |
|---|---|
|  | Two infinitely long plates of width L, joined along one of the long edges:<br><br>$$F_{1-2} = F_{2-1} = 1 - \sin\frac{\alpha}{2}$$ |
|  | Two infinitely long plates of different widths (H, L), joined along one of the long edges and with a 90° angle between them:<br><br>$$F_{1-2} = \frac{1}{2}[1 + x - (1 + x^2)^{1/2}]$$<br><br>where x = H/L |
|  | Triangular cross-section enclosure formed by three infinitely long plates of different widths $(L_1, L_2, L_3)$:<br><br>$$F_{1-2} = \frac{L_1 + L_2 - L_3}{2L_1}$$ |
|  | Circular disk and plane element positioned on the disc centerline:<br><br>$$F_{1-2} = \frac{R^2}{H^2 + R^2}$$ |
|  | Parallel discs positioned on the same centerline:<br><br>$$F_{1-2} = \frac{1}{2}\left\{ X - \left[ X^2 - 4\left(\frac{x_2}{x_1}\right)^2 \right]^{1/2} \right\}$$<br><br>where<br><br>$$x_1 = \frac{R_1}{H}, \; x_2 = \frac{R_2}{H}, \text{ and } X = 1 + \frac{1 + x_2^2}{x_1^2}$$ |
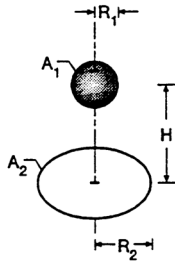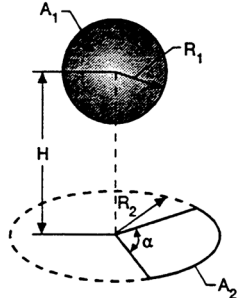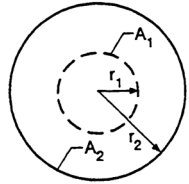
**TABLE 2.1.10 (continued)** Minicatalog of Geometric View Factors

| Configuration | Geometric View Factor |
|---|---|
|  | Infinite cylinder parallel to an infinite plate of finite width ($L_1$ - $L_2$): $$F_{1\text{-}2} = \frac{R}{L_1 - L_2}\left(\tan^{-1}\frac{L_1}{H} - \tan^{-1}\frac{L_2}{H}\right)$$ |
|  | Two parallel and infinite cylinders: $$F_{1\text{-}2} = F_{2\text{-}1} = \frac{1}{\pi}\left[\left(X^2 - 1\right)^{1/2} + \sin^{-1}\left(\frac{1}{X}\right) - X\right]$$ where $X = 1 + \dfrac{L}{2R}$ |
|  | Concentric cylinders of infinite length: $$F_{1\text{-}2} = 1$$ $$F_{2\text{-}1} = \frac{R_1}{R_2}$$ $$F_{2\text{-}2} = 1 - \frac{R_1}{R_2}$$ |
|  | Row of equidistant infinite cylinders parallel to an infinite plate: $$F_{1\text{-}2} = 1 - (1 - x^2)^{1/2} + x\,\tan^{-1}\left[\frac{1 - x^2}{x^2}\right]^{1/2}$$ where $x = D/L$ |

where $q_{\text{conv,i}} = h_i\,(T_{\text{ap}} - T_{\text{cp}})$ is the convection heat exchange between the absorber plate and the cover plate and $q_{\text{rad,ap-cp}} = \sigma\left(T_{ap}^4 - T_{cp}^4\right)\big/\left(1/\varepsilon_{ap} + 1/\varepsilon_{cp} - 1\right)$ is the heat exchange by radiation between them. Note that the shape factor between two parallel plates is equal to one. The left-hand side of Eq. (2.1.64) represents the solar irradiation transmitted through the cover plate and absorbed by the absorber plate. Substituting for $q_{\text{conv,i}}$ and $q_{\text{rad,ap-cp}}$ in Eq. (2.1.64), we obtain (for $\alpha_{\text{ap,s}} = 1$)

$$\tau_{cp,s}\; G_s = h_i\left(T_{ap} - T_{cp}\right) + \frac{\sigma\left(T_{ap}^4 - T_{cp}^4\right)}{1/\varepsilon_{ap} + 1/\varepsilon_{cp} - 1} + q_u. \tag{2.1.65}$$

**TABLE 2.1.10 (continued)** Minicatalog of Geometric View Factors

| Configuration | Geometric View Factor |
|---|---|
| | Sphere and disc positioned on the same centerline:<br><br>$$F_{1\text{-}2} = \frac{1}{2}\left[1 - \frac{1}{\sqrt{1+x^2}}\right]$$<br><br>where $x = \dfrac{R_2}{H}$ |
| | Sphere and a sector of disk positioned on the same centerline:<br><br>$$F_{1\text{-}2} = \frac{\alpha}{4\pi}\left[1 - \frac{1}{\sqrt{1+x^2}}\right]$$<br><br>where $x = \dfrac{R_2}{H}$ |
| | Concentric spheres:<br><br>$$F_{1\text{-}2} = 1$$<br><br>$$F_{2\text{-}1} = \left(\frac{R_1}{R_2}\right)^2$$<br><br>$$F_{2\text{-}2} = 1 - \left(\frac{R_1}{R_2}\right)^2$$ |

To find $q_u$ from Eq. (2.1.65), $T_{cp}$ should be known, which is obtained from an energy balance on the cover plate, as in :

$$\alpha_{cp,s}\ G_s + q_{conv,i} + q_{rad,ap-cp} = q_{conv,o} + q_{rad,cp-sky}, \tag{2.1.66}$$

where $q_{conv,o} = h_o\,(T_{cp} - T_\infty)$ is the heat loss by convection and $q_{rad,cp-sky} = \varepsilon_{cp}\sigma\left(T_{cp}^4 - T_{sky}^4\right)$ is the heat exchange by radiation between the cover plate and sky. Equation (2.1.66) can be written as

$$\alpha_{cp,s}\ G_s + h_i\left(T_{ap} - T_{cp}\right) + \frac{\sigma\left(T_{ap}^4 - T_{cp}^4\right)}{1/\varepsilon_{ap} + 1/\varepsilon_{cp} - 1} = h_o\left(T_{cp} - T_\infty\right) + \varepsilon_{cp}\ \sigma\left(T_{cp}^4 - T_{sky}^4\right). \tag{2.1.67}$$

Substituting for known quantities in Eq. (2.1.67) $T_{cp}$ is calculated to be $T_{cp} = 44.6°C$. Substituting for $T_{cp}$ and other known quantities in Eq. (2.1.65), $q_u$ is 402.5 W/m².
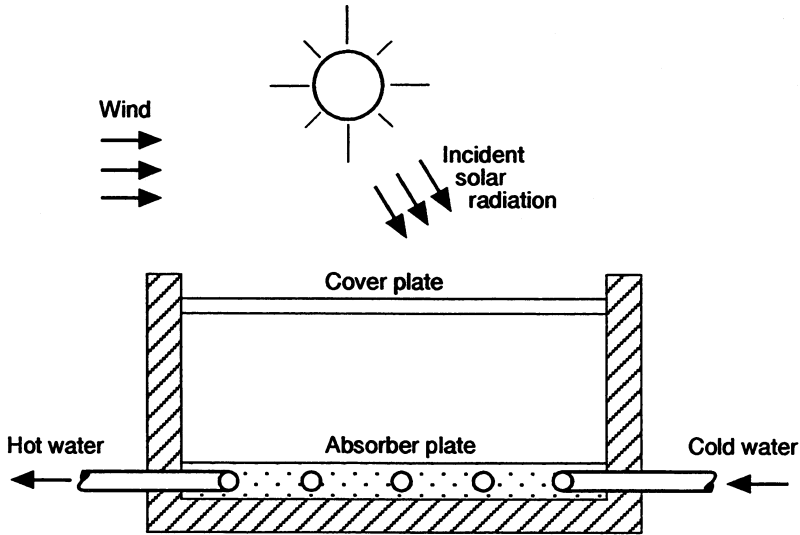
**FIGURE 2.1.29**   Flat-plate solar collector with a single glass cover.
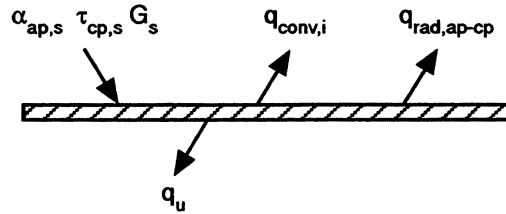


**FIGURE 2.1.30**   Energy balance on a unit area of the absorber plate.
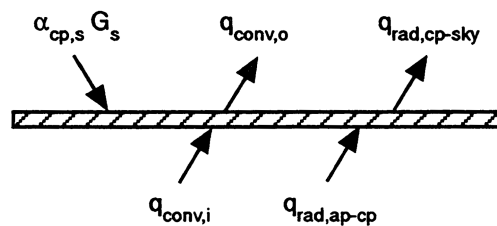


**FIGURE 2.1.31**   Energy balance on a unit area of the cover plate.

## 2.1.3   Fundamentals of Fluid Mechanics

The distribution of heated and cooled fluids by pipes and ducts, is an essential part of all HVAC processes and systems. The fluids encountered in these processes are gases, vapors, liquids, or mixtures of liquid and vapor (2–phase flow). This section briefly reviews certain basic concepts of fluid mechanics that are often encountered in analyzing and designing HVAC systems.

Fluid flowing through a conduit will encounter shear forces that result from viscosity of the fluid. The fluid undergoes continuous deformation when subjected to these shear forces. Furthermore, as a result of shear forces, the fluid will experience pressure losses as it travels through the conduit.
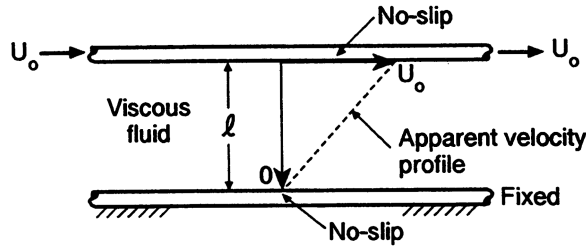
**FIGURE 2.1.32** A fluid sheared between two parallel plates.

**Viscosity**, μ, is a property of fluid best defined by Newton's Law of Viscosity:

$$\tau = \mu \frac{du}{dy}, \tag{2.1.68}$$

where $\tau$ is the frictional shear stress, and $du/dy$ represents the measure of the motion of one layer of fluid relative to an adjacent layer. The following observation will help to explain the relationship between viscosity and shear forces. Consider two very long parallel plates with a fluid between them, as shown in Figure 2.1.32. Assume a uniform pressure throughout the fluid. The upper plate is moving with a constant velocity $u_0$, and the lower plate is stationary. Experiments show that the fluid adjacent to the moving plate will adhere to that plate and move along with the plate at a velocity equal to $u_0$, whereas the fluid adjacent to the stationary plate will have zero velocity. The experimentally verified velocity distribution in the fluid is linear and can be expressed as

$$u = \frac{y}{\ell} \, u_0, \tag{2.1.69}$$

where $\ell$ is the distance between the two parallel plates. The force necessary to keep the upper plate moving at a constant velocity if $u_0$ should be large enough to overcome (or balance) the frictional forces in the fluid. Again, experimental observations indicate that this force is proportional to the ratio $u_0/\ell$. One can conclude from Eq. (2.1.69) that $u_0/\ell$ is equal to the rate of change of velocity, $du/dy$. Therefore, the frictional force per unit area (shear stress), $\tau$, is proportional to $du/dy$, and the proportionality constant is μ, which is a property of the fluid known as viscosity. Therefore, we obtain Eq. (2.1.68), which is known as Newton's Law of Viscosity (or friction). The quantity μ is a measure of the viscosity of the fluid and depends on the temperature and pressure of the fluid. Equation (2.1.68) is analogous to Fourier's Law of Heat Conduction given by Eq. (2.1.25). Fluids that do not obey Newton's Law of Viscosity are called non-Newtonian fluids. Fluids with zero viscosity are known as inviscid or ideal fluids. Molasses and tar are examples of highly viscous liquids; water and air on the other hand, have low viscosities. The viscosity of a gas increases with temperature, but the viscosity of a liquid decreases with temperature. Reid, Sherwood, and Prausnitz [1977] provide a thorough discussion on viscosity.

## Flow Characteristics

The flow of a fluid may be characterized by one or a combination of the following descriptor pairs: laminar/turbulent, steady/unsteady, uniform/nonuniform, reversible/irreversible, rotational/irrotational. In this section, however, we will focus our attention only on laminar and turbulent flows.

In **laminar flow**, fluid particles move along smooth paths in layers, with one layer sliding smoothly over an adjacent layer without significant macroscopic mixing. Laminar flow is governed by Newton's Law of Viscosity. Turbulent flow is more prevalent than laminar flow in engineering processes. In

**turbulent flow**, the fluid particles move in irregular paths, causing an exchange of momentum between various portions of the fluid; adjacent fluid layers mix and this mixing mechanism is called eddy motion. In this type of flow, the velocity at any given point under steady-state conditions fluctuates in all directions about some time-mean value. Turbulent flow causes greater shear stresses throughout the fluid, producing more irreversibilities and losses. An equation similar to Newton's Law of Viscosity may be written for turbulent flows:

$$\tau = (\mu + \eta) \ \frac{du}{dy}, \tag{2.1.70}$$

where the factor $\eta$ is the eddy viscosity, which depends on the fluid motion and density. Unlike the fluid viscosity, $\mu$, the eddy viscosity is not a fluid property and is determined through experiments.

The type of flow is primarily determined by the value of a nondimensional number known as a Reynolds number, which is the ratio of inertia forces to viscous forces given by

$$Re = \frac{\rho \ u_{avg} \ D_H}{\mu}, \tag{2.1.71}$$

where $u_{avg}$ is the average velocity and $D_H$ is the hydraulic diameter defined by Eq. (2.1.50). The value of the Reynolds number can be used as the criterion to determine whether the flow is laminar or turbulent. In general, laminar flow occurs in closed conduits when $Re < 2,100$; the flow goes through transition when $2,100 < Re < 6,000$ and becomes turbulent when $Re > 6,000$.

For fluid flow over flat plates, laminar flow is generally accepted to occur at $Re_x = \rho u x / \mu < 3 \times 10^5$, where $x$ is the distance from the leading edge of the plate and $u$ is the free-stream velocity. Note that if the flow approaching the flat plate is turbulent, it will remain turbulent from the leading edge of the plate forward.

When a fluid is flowing over a solid surface, the velocity of the fluid layer in the immediate neighborhood of the surface is influenced by viscous shear; this region of the fluid is called the **boundary layer**. Boundary layers can be laminar or turbulent depending on their length, the fluid viscosity, the velocity of the bulk fluid, and the surface roughness of the solid body.

### Analysis of Flow Systems

Most engineering problems require some degree of system analysis. Regardless of the nature of the flow, all fluid-flow situations are subject to the following relations:

1. Newton's Law of Motion, $\Sigma F = \dfrac{1}{g_c} \dfrac{d(mu)}{dt}$
2. Conservation of mass
3. The First and Second Laws of Thermodynamics
4. Boundary conditions such as zero velocity at a solid surface.

In an earlier section, the First Law of Thermodynamics was applied to a system shown in Figure 2.1.1. With some modifications, the same energy balance can be applied to any fluid-flow system. For example, a term representing the frictional pressure losses should be added to the left-hand side of Eq. (2.1.2), as expressed by the following equation:

$$e_2 + \frac{u_2^2}{2g_c} + \frac{gz_2}{g_c} + \frac{p_2}{\rho_2} + \frac{\dot{w}_f}{\dot{m}} = e_1 + \frac{u_1^2}{2g_c} + \frac{gz_1}{g_c} + \frac{p_1}{\rho_1} + \frac{\dot{Q} + \dot{w}}{\dot{m}}, \tag{2.1.72}$$

where $\dot{w}_f$ represents the frictional pressure losses and is the rate of work done on the fluid (note the sign change from $-\dot{w}$ to $+\dot{w}$ in Eq. (2.1.72), because the work is done on the fluid). In the remainder of this section, we will focus on obtaining an expression for $\dot{w}_f$ and analyzing different sources of frictional pressure losses.

Using Newton's Law of Motion, the weight of a body, $w$, can be defined as the force exerted on the body as a result of the acceleration of gravity, $g$,

$$w = \frac{g}{g_c} m. \tag{2.1.73}$$

In the English system of units, 1 lbm weighs 1 lbf at sea level because the proportionality constant $g_c$ is numerically equal to the gravitational acceleration (32.2 ft/s²). However, in the SI system, 1 kg of mass weighs 9.81 N at sea level because $g_c = 1$ kg m/N s² (or $g_c = 10^3$ kg m³/kJ s²) and g = 9.81 m/s².

Equation (2.1.73) can be used to determine the static pressure of a column of fluid. For example, a column of fluid at height $z$ that experiences an environment or atmospheric pressure of $p_0$ over its upper surface will exert a pressure of $p$ at the base of the fluid column given by

$$p = p_0 + \rho z \frac{g}{g_c}, \tag{2.1.74}$$

where $\rho$ is the density of the fluid. The base pressure as expressed by Eq. (2.1.74) is a function of fluid height or fluid head and does not depend on the shape of the container. Knowing the fluid head is very important, especially in specifying a pump, as it is common practice to specify the performance of the pump in terms of fluid head. Therefore, we can calculate the required mechanical power from

$$\dot{w}_{pump} = zg\, \dot{m}. \tag{2.1.75}$$

Equation (2.1.75) expresses the pump power at 100% efficiency; in reality, however, mechanical pumps have efficiencies of less than 100%. Therefore, the required mechanical power $\dot{w}$ is

$$\dot{w} = \frac{\dot{w}_{pump}}{\eta_{pump}}. \tag{2.1.76}$$

A pump used in a system is expected to overcome various types of pressure losses such as frictional pressure losses in the piping; pressure losses due to fittings, bends, and valves; and pressure losses due to sudden enlargements and contractions. All these pressure losses should be calculated for a system and summed up to obtain the total pressure drop through a system.

The frictional pressure losses in the piping are caused by the shearing force at the fluid-solid interface. Through a force balance, we can obtain the frictional pressure loss of an incompressible fluid in a pipe between two points as

$$p_1 - p_2 = 4f\, \frac{L}{D}\, \frac{\rho u^2}{2g_c}, \tag{2.1.77}$$

where L is the length of the pipe between points 1 and 2, $D$ is the pipe diameter, $u$ is the average fluid velocity in the pipe, and $f$ is the dimensionless friction factor. For laminar flow inside a pipe, the friction factor is

$$f = \frac{16}{\mathrm{Re}_{D_H}}, \tag{2.1.78}$$

where the Reynolds number is based on the hydraulic diameter $D_H$. The friction factor for turbulent flow depends on the surface roughness of the pipe and on the Reynolds number. The friction factor for various surface roughnesses and Reynolds numbers is presented in Figure 2.1.33, which is called the **Moody diagram**. The relative roughnesses of the various commercial pipes are given in Figure 2.1.34.

**VALUES OF (vd) FOR WATER AT 15°C (VELOCITY IN m/s X DIAMETER IN mm)**
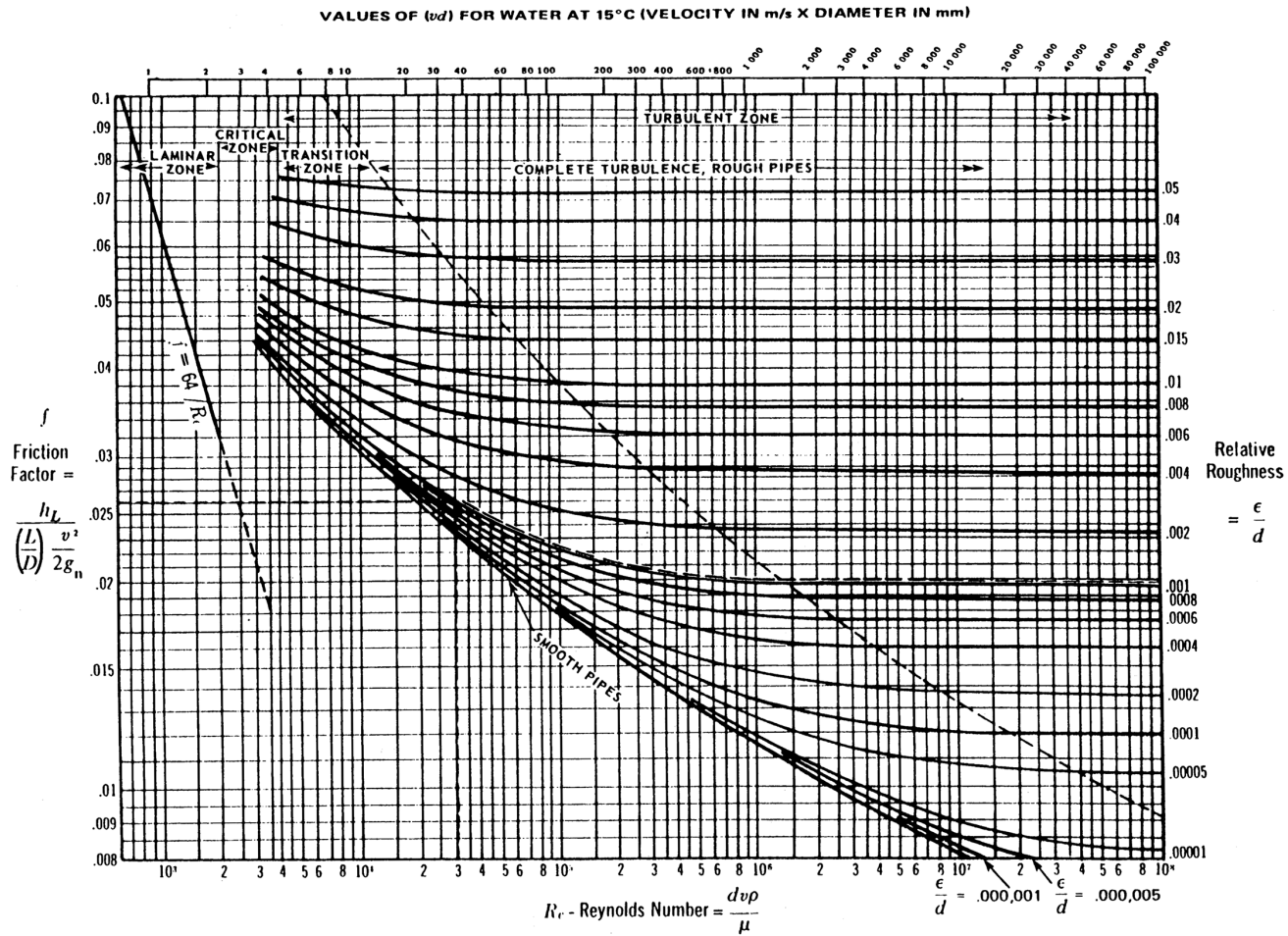


**FIGURE 2.1.33**  Friction factors for various surface roughness and Reynolds numbers. Data extracted from *Friction Factor for Pipe Flow* by L.F. Moody (1944), with permission of the publisher, The American Society of Mechanical Engineers.
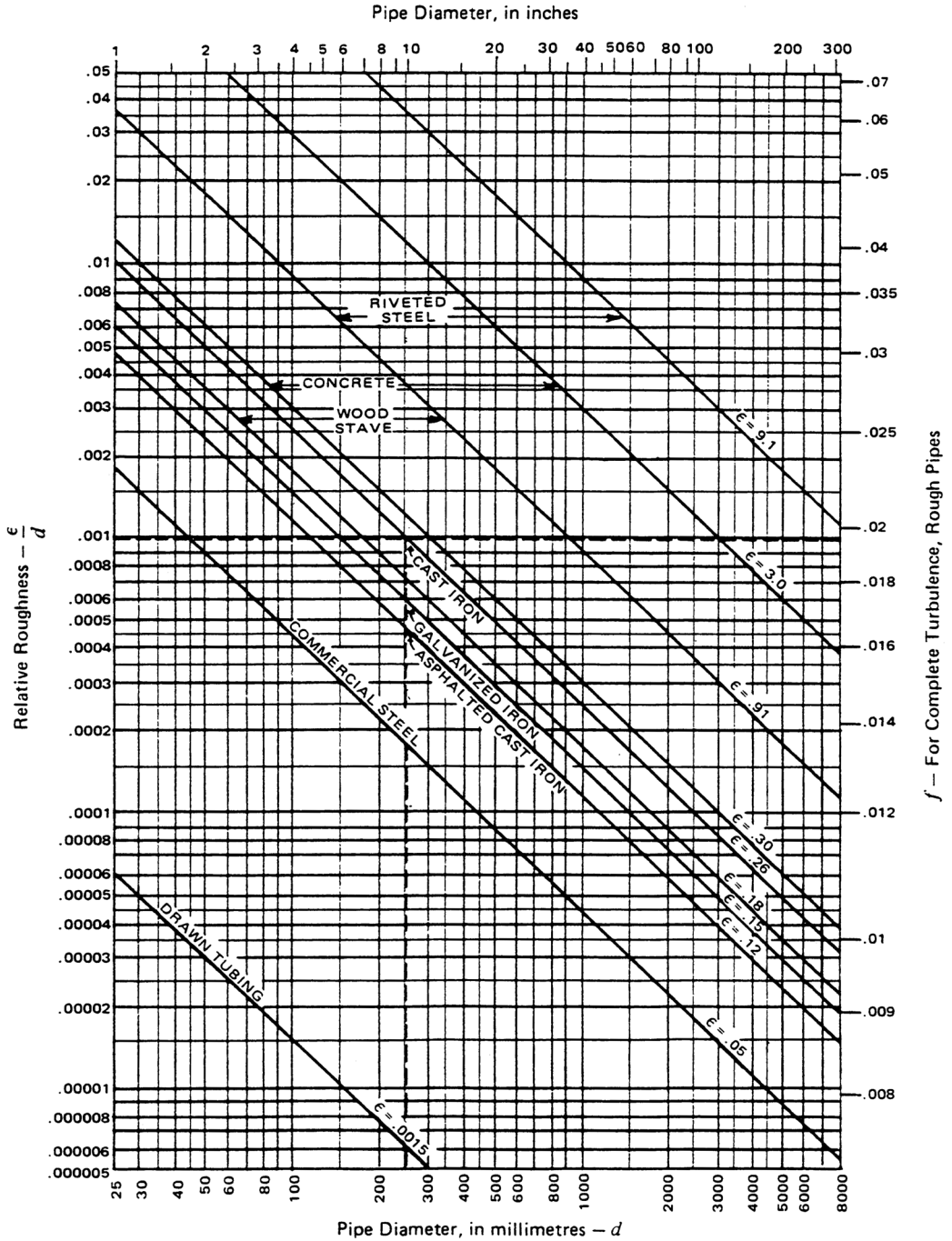
**FIGURE 2.1.34** Relative roughness of commercial pipe. Data extracted from *Friction Factor for Pipe Flow* by L.F. Moody (1944), with permission of the publisher, The American Society of Mechanical Engineers.

Pressure losses due to fittings, bends, and valves are generally determined through experiments. This type of pressure loss can be correlated to the average fluid velocity in the pipe by

$$\Delta p_b = k_b \frac{\rho u^2}{2g_c}, \tag{2.1.79}$$

where $k_b$ is a pressure-loss coefficient obtained from a handbook or from the manufacturer, and $u$ is the average fluid velocity in the pipe upstream of the fitting, bend, or valve. For typical values of $k_b$, refer to Perry, Perry, Chilton, and Kirkpatrick [1963], Freeman [1941], and the *Standards of Hydraulic Institute* [1948].

Pressure losses due to sudden enlargement of the cross section of the pipe can be calculated using

$$\Delta p = \alpha \left(1 - \frac{A_s}{A_L}\right) \frac{\rho u^2}{2g_c} = k_e \frac{\rho u^2}{2g_c}, \tag{2.1.80}$$

where $A_s/A_L$ is the ratio of the cross-sectional area of the smaller pipe to that of the larger pipe, $\alpha$ is the nondimensional pressure-loss coefficient ($\alpha = 1$ for turbulent flow and 2 for laminar flow), and $u$ is the average fluid velocity in the smaller pipe. Note that a gradual increase in pipe cross section will have little effect on pressure losses. In case of sudden contraction of pipe size, the pressure drop can be calculated from

$$\Delta p = 0.55 \, \alpha \left(1 - \frac{A_s}{A_L}\right) \frac{\rho u_c^2}{2g_c} = k_c \frac{\rho u_c^2}{2g_c}, \tag{2.1.81}$$

where $A_s/A_L$ and $\alpha$ are as defined for Eq. (2.1.80), and $u_c$ is the average fluid velocity in the smaller pipe (contraction). Adding the various pressure losses, the total pressure loss in a system can be calculated from

$$\frac{\dot{w}_f}{\dot{m}} = \Sigma \frac{\Delta p}{\rho} = 4f \frac{L}{D} \frac{u^2}{2g_c} + \Sigma k_b \frac{u^2}{2g_c} + k_e \frac{u^2}{2g_c} + k_c \frac{u_c^2}{2g_c}. \tag{2.1.82}$$

For a system under consideration, a pump must be chosen that can produce sufficient pressure head to overcome all the losses presented in Eq. (2.1.82). For system engineering applications, Eq. (2.1.82) can be simplified to

$$\frac{\dot{w}_f}{\dot{m}} = \Sigma \frac{2fLu^2}{g_c D}, \tag{2.1.83}$$

where $f$ is as defined for Eq. (2.1.77), $u$ is the average velocity inside the conduit, and $D$ is the appropriate diameter for the section of the system under consideration. The summation accounts for the effect of changes in pipe length, diameter, and relative roughness. The length L represents not only the length of the straight pipe of the system, but also, equivalent lengths of straight pipe that would have the same effects as the fittings, bends, valves, and sudden enlargements or contractions. Figure 2.1.35 provides a nomogram to determine such equivalent lengths.

### Example 2.1.10

Figure 2.1.36 shows a system layout for a small solar collector where water at 35°C (95°F) is pumped from a tank (surface-area heat exchanger) through three parallel solar collectors and back to the tank. The water flow rate is 0.9 m³/min (23.8 gal/min). All the piping is 1–in. Sch 40 steel pipe (cross-sectional area = 0.006 ft² = $5.57 \times 10^{-4}$ m², with inside diameter = 1.049 in. = 0.0266 m). The pressure drop through each solar collector is estimated to be 1.04 kPa (0.15 psi) for a flow rate of 0.03 m³/min
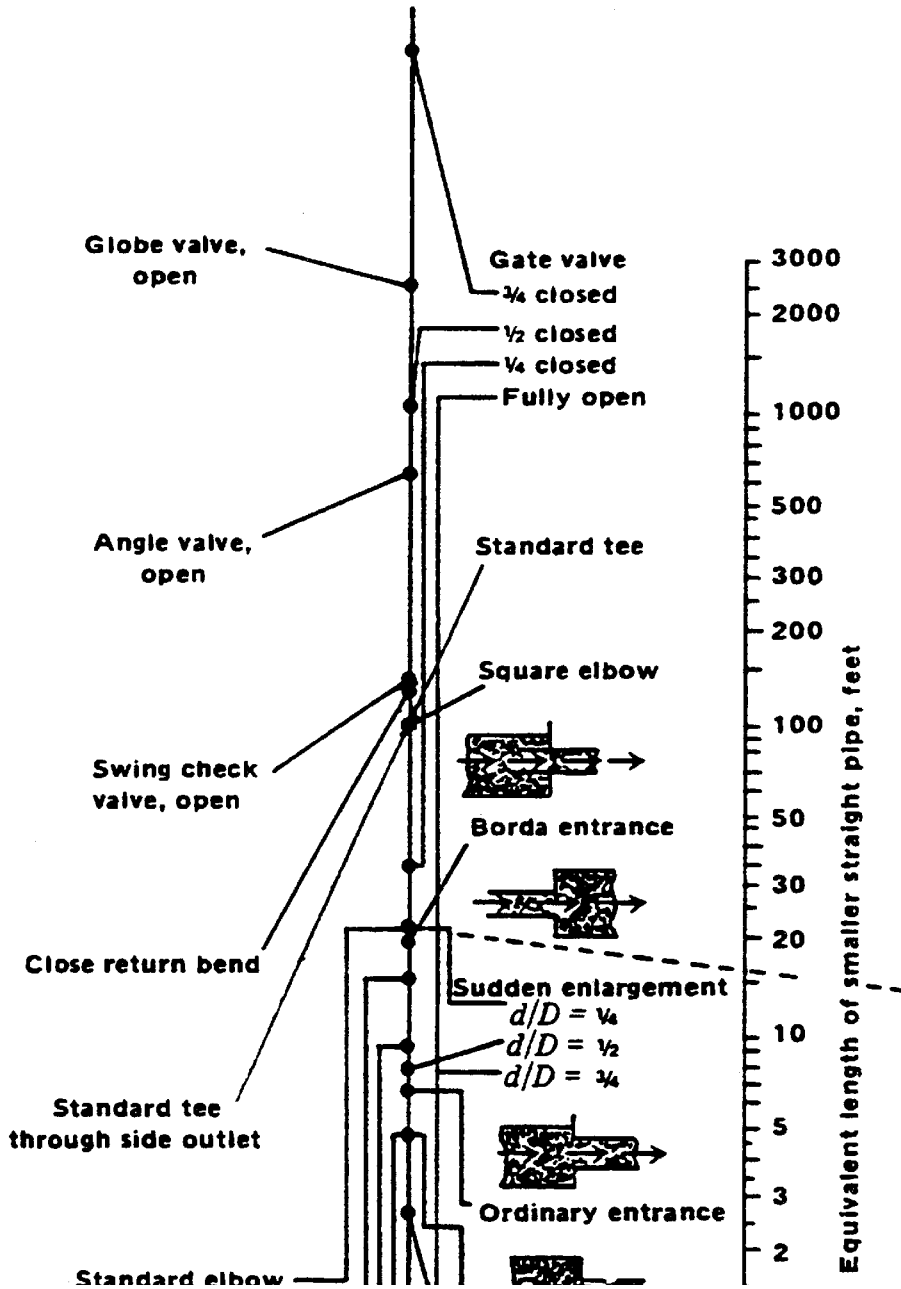
**FIGURE 2.1.35** Equivalent lengths for friction losses. Data extracted from *Flow of Fluids through Valves, Fittings and Pipe,* Publication 410M (1988), with permission of the publisher, Crane Company.

(7.9 gal/min). Find the appropriate pump size for this system using the lengths and fittings specified in Figure 2.1.36. Assume a pump efficiency of about 75% and that the heat gain through the collectors is equal to the change in the internal energy of the water from point 1 to point 2.

*Solution:*

To find the pump 1 size, we apply an energy-balance similar to Eq. (2.1.72) between points 1 and 2 shown in Figure 2.1.36. Point 1 represents the water free-surface in the tank, whereas point 2 represents

**FIGURE 2.1.36**    Layout of a small solar-collector system.

the water inlet to the tank after the water has circulated through the collectors. Because both points (1 and 2) have the same pressure, we have

$$\frac{\Delta p_{2-1}}{\rho} = \frac{p_2}{\rho_2} - \frac{p_1}{\rho_1} = 0.$$

Similarly, because there is no significant height difference between these two points, we have

$$\frac{g}{g_c} \Delta z_{2-1} = \frac{g z_2}{g_c} - \frac{g z_1}{g_c} = 0.$$

The velocity at the water free-surface (point 1) is $u_1 = 0$. For point 2, the velocity is

$$u_2 = \frac{q_2}{A_2} = \frac{0.09 \text{ m}^3/\text{min}}{5.57 \times 10^{-4} \text{ m}^2} = 161.6 \text{ m/min} = 2.7 \text{ m/s}.$$

Therefore,

$$\frac{\Delta u_{2-1}^2}{2 g_c} = \frac{u_2^2}{2 g_c} - \frac{u_1^2}{2 g_c} = \frac{\left(2.7 \text{ m/sec}\right)^2}{2 \left(10^3 \dfrac{\text{kg}}{\text{kJ}} \dfrac{\text{m}^2}{\text{sec}^2}\right)} = 3.7 \times 10^{-3} \text{ kJ/kg}.$$

Also note that

$$\Delta e_{2-1} = e_2 - e_1 = \frac{\dot{Q}}{\dot{m}}.$$

Therefore, Eq. (2.1.72) reduces to

$$\frac{\Delta u_{2-1}^2}{2 g_c} + \frac{\dot{w}_f}{\dot{m}} = \frac{\dot{w}}{\dot{m}}. \tag{2.1.84}$$

The frictional pressure losses $\dot{w}_f$ should be determined for the whole system between points 1 and 2. Equation (2.1.83) can be used to determine $\dot{w}_f$; however, the total equivalent length should be determined first. The tot al straight piping in the system is

$$L_s = 2 \text{ m} + 2 \text{ m} + 1 \text{ m} + 1 \text{ m} + 8 \text{ m} + 1 \text{ m} + 5 \text{ m} + 8 \text{ m} = 28 \text{ r}$$

Using Figure 2.1.35, the equivalent lengths for bends and valves are obtained as follows:

Borda entrance: 0.79 m (2.6 ft)
Open gate valve: 0.18 m (0.6 ft)
Open globe valve: 7.90 m (26.0 ft)
Standard tee: 1.80 m (5.9 ft)
Standard elbow: 0.81 m (2.7 ft)

Therefore, with two standard elbows in this system, the equivalent length for bends, elbows, and valves becomes $L_b$ = 0.79 m + 0.18 m + 7.9 m + 1.8 m + 2 (0.82 m) = 12.31 m, and the total equivalent of 1–in. Sch 40 pipe is L = $L_b$ + $L_s$ = 40.31 m. To calculate the friction factor, we must calculate the Reynolds number. Assuming an average fluid density of $\rho$ = 988 kg/m³ and an absolute viscosity of $\mu$ = $555 \times 10^{-6}$ Ns/m², the Reynolds number is

$$\text{Re} = \frac{\rho u D_H}{\mu} = \frac{988 \text{ kg}/\text{m}^3 \times 2.7 \text{ m}/\text{s} \times 0.0266 \text{ m}}{555 \times 10^{-6} \text{ N s}/\text{m}^2} = 128 \times 10^3.$$

From Figure 2.1.34, the relative roughness of the pipe obtained is $e/D$ = 0.0018, and by using Figure 2.1.33 (the Moody diagram), the friction factor obtained is $f \approx 0.006$. Substituting in Eq. (2.1.83), the work required to overcome the frictional losses is obtained from

$$\frac{\dot{w}_f}{\dot{m}} = \frac{2 f L u^2}{g_c D} + Fr_c,$$

where $Fr_c$ is the required work to overcome pressure loss through the collectors. Since the collectors are in parallel, the total pressure loss is equal to the pressure drop through each collector. Therefore,

$$Fr_c = 1.04 \text{ } kN/\text{m}^2 \times \frac{1}{988 \text{ kg}/\text{m}^3} = 0.0011 \text{ kJ}/\text{kg},$$

and

$$\frac{\dot{w}_f}{\dot{m}} = \frac{2 \times 0.006 \times 40.31 \text{ m} \times (2.7 \text{ m}/\text{s})^2}{10^3 \text{ } \frac{\text{kg}}{\text{kJ}} \frac{\text{m}^2}{\text{s}^2} \times 0.0266 \text{ m}} + 0.0011 \text{ kJ}/\text{kg} = 0.134 \text{ kJ}/\text{kg}.$$

Substituting for $\frac{\Delta u_{2-1}^2}{2g_c}$ and $\dot{w}_f$ in Eq. (2.1.84), we can calculate the input power to the pump (the mass flow rate of the fluid is 0.494 kg/s):

$$\frac{\dot{w}}{\dot{m}} = \frac{\Delta u_{2-1}^2}{2g_c} + \frac{\dot{w}_f}{\dot{m}} = 3.7 \times 10^{-3} \text{ kJ}/\text{kg} + 0.134 \text{ kJ}/\text{kg} = 0.138 \text{ kJ}/\text{kg}.$$

With a 75% efficiency, the actual mechanical energy required will be

$$w_{\text{act}} = \frac{0.138 \ \text{kJ/kg}}{0.75} = 0.184 \ \text{kJ/kg}.$$

The appropriate pump size is

$$\dot{w}_{\text{act}} = 0.184 \ \text{kJ/kg} \times 0.494 \ \text{kg/s} = 0.091 \ \text{kJ/s} = 0.12 \ \text{hp}.$$

## 2.1.4 Heat Exchangers

A **heat exchanger** is a device designed to transfer energy between two fluids. Heat exchangers are often used to transfer thermal energy from a source (e.g., a boiler or chiller) to a point of use (e.g., a cooling or heating coil). They are particularly important for improving overall process efficiency of energy-efficient systems. Heat exchangers can be expensive and must be designed carefully to maximize effectiveness and minimize cost. Depending on their application, heat exchangers can have different shapes, designs, and sizes. The major types of heat exchangers include boilers, condensers, radiators, evaporators, cooling towers, regenerators, and recuperators. All heat exchangers are identified by their geometric shape and the direction of flow of the heat-transfer fluids inside them. Figure 2.1.37 depicts some common heat exchangers. In the following paragraphs, we describe the operating principles of some of the more common heat exchangers.

A **direct-contact heat exchanger** is designed so that two fluids are physically brought into contact, with no solid surface separating them. In this type of heat exchanger, fluid streams form a mutual interface through which the heat transfer takes place between the two fluids. Direct-contact (DC) heat exchangers are best used when the temperature difference between the hot and cold fluids is small. An example of a direct-contact heat exchanger is a cooling tower, where water and air are brought together by letting water fall from the top of the tower and having it contact a stream of air flowing upward. Evaporative coolers are another common DC device.

**Regenerators** are heat exchangers in which the hot and cold fluids flow alternately through the same space. As a result of alternating flow, the hot fluid heats the core of the heat exchanger, where the stored heat is then transferred to the cold fluid. Regenerators are used most often with gas streams, where some mixing of the two streams is not a problem and where the cost of another type of heat exchanger would be prohibitive. For example, heat recovery in very energy efficient homes is often done with "air-to-air" regenerators to maintain an acceptable quality of air inside the homes.

The **recuperator** is the heat exchanger encountered most often. It is designed so that the hot and cold fluids do not come into contact with each other. Energy is exchanged from one fluid to a solid surface by convection, through the solid by conduction, and from the other side of the solid surface to the second fluid by convection. The evaporator tube bundle in a chiller is such as device.

In Section 2.1.2, we described these heat-transfer processes and developed some simple equations that are applied here to determine basic equipment performance. Designing a heat exchanger also requires estimating the pressure flow losses that can be carried out, based on the information provided in Section 2.1.3. Finally, appropriate materials must be selected and a structural analysis done; Frass and Ozisik [1965] provide a good discussion of these topics.

### Heat-Exchanger Performance

The performance of a heat exchanger is based on the exchanger's ability to transfer heat from one fluid to another. Calculating the heat transfer in heat exchangers is rather involved because the temperature of one or both of the fluids is changing continuously as they flow through the exchanger. There are three main flow configurations in heat exchangers: parallel flow, counter flow, and cross flow. In **parallel-flow** heat exchangers, both fluids enter from one end of the heat exchanger flowing in the same direction and they both exit from the other end. In **counter-flow** heat exchangers, hot fluid enters from one end and flows in an opposite direction to cold fluid entering from the other end. In **cross-flow** heat exchangers, baffles are used to force the fluids to move perpendicular to each other, to take advantage of higher heat-transfer coefficients encountered in a cross-flow configuration. Figure 2.1.38 shows the
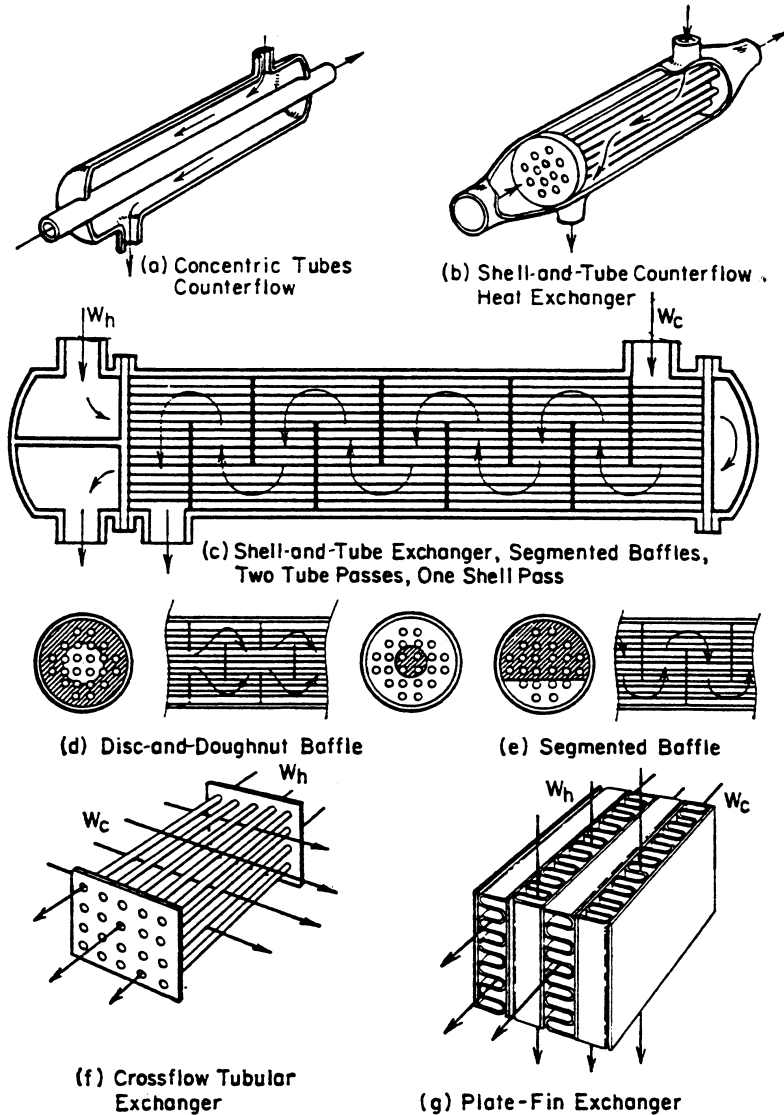
**FIGURE 2.1.37** Some examples of heat exchangers.

temperature variation of the fluids inside the heat exchanger for a parallel-flow and a counter-flow heat exchanger. In parallel-flow heat exchangers, the temperature difference $\Delta T_i$ between the two fluids at the inlet of the heat exchanger is much greater than $\Delta T_o$, the temperature difference at the outlet of the heat exchanger. In counter-flow heat exchangers, however, the temperature difference between the fluids shows only a slight variation along the length of the heat exchanger. Assuming that the heat loss from the heat exchanger is negligible, usually the case in a practical design, the heat loss of the hot fluid should be equal to the heat gain by the cold fluid. Therefore, we can write

$$\dot{Q} = \dot{m}_c c_{p,c} \left( T_{co} - T_{ci} \right) = \dot{m}_h c_{p,h} \left( T_{hi} - T_{ho} \right), \tag{2.1.85}$$

where the subscripts $c$ and h refer to cold and hot fluids, respectively. Note that in heat-exchanger analysis, the terms $\dot{m}_c c_{p,c}$ and $\dot{m}_h c_{p,h}$ are called the **capacity rates** of the cold and hot fluids, respectively, and are usually represented by $C_c$ and $C_h$.